Molecular Therapy
Original Article

Pre-clinical Gene Therapy with AAV9/*AGA* in Aspartylglucosaminuria Mice Provides Evidence for Clinical Translation

Xin Chen,[1] Sarah Snanoudj-Verber,[2] Laura Pollard,[3] Yuhui Hu,[1] Sara S. Cathey,[3] Ritva Tikkanen,[4] and Steven J. Gray[1]

[1]Department of Pediatrics, UTSW Medical Center, Dallas, TX 75390, USA; [2]Metabolic Biochemistry, University Hospital of Rouen, Rouen, France; [3]Greenwood Genetics Center, Greenwood, SC 29646, USA; [4]Institute of Biochemistry, Medical Faculty, University of Giessen, Giessen, Germany

Aspartylglucosaminuria (AGU) is an autosomal recessive lysosomal storage disease caused by loss of the enzyme aspartylglucosaminidase (AGA), resulting in AGA substrate accumulation. AGU patients have a slow but progressive neurodegenerative disease course, for which there is no approved disease-modifying treatment. In this study, AAV9/*AGA* was administered to *Aga*$^{-/-}$ mice intravenously (i.v.) or intrathecally (i.t.), at a range of doses, either before or after disease pathology begins. At either treatment age, AAV9/*AGA* administration led to (1) dose dependently increased and sustained AGA activity in body fluids and tissues; (2) rapid, sustained, and dose-dependent elimination of AGA substrate in body fluids; (3) significantly rescued locomotor activity; (4) dose-dependent preservation of Purkinje neurons in the cerebellum; and (5) significantly reduced gliosis in the brain. Treated mice had no abnormal neurological phenotype and maintained body weight throughout the whole experiment to 18 months old. In summary, these results demonstrate that treatment of *Aga*$^{-/-}$ mice with AAV9/*AGA* is effective and safe, providing strong evidence that AAV9/*AGA* gene therapy should be considered for human translation. Further, we provide a direct comparison of the efficacy of an i.v. versus i.t. approach using AAV9, which should greatly inform the development of similar treatments for other related lysosomal storage diseases.

INTRODUCTION

Aspartylglucosaminuria (AGU) is an autosomal recessive inherited lysosomal storage disease caused by the loss of functional aspartylglucosaminidase (AGA) enzyme.[1] The AGA enzyme is required for the breakdown of glycoproteins within cellular lysosomes. Most individuals with a mutated *AGA* gene produce either small quantities of defective protein or an inactive precursor polypeptide, which results in the accumulation of the AGA substrate (aspartylglucosamine, GlcNAc-Asn) in the lysosomes of all tissues and body fluids. The accumulated substrate GlcNAc-Asn is excreted in urine of patients in large quantities.

AGU is a slow but progressive and severe neurodegenerative disease characterized by intellectual disability, skeletal and motor abnormalities, and early mortality.[1,2] The median lifespan of AGU patients is approximately 30 to 40 years. The major consequence of substrate accumulation is lysosomal hypertrophy that manifests as intellectual disability as well as additional symptoms including skeletal and joint abnormalities. AGU patients have developmental delays including delayed speech and impaired learning caused by progressive brain atrophy. By the third decade of life, patients have severe intellectual and physical disabilities and are highly dependent on supportive care.

There is no approved therapy for AGU patients that targets the root cause of the disease. A few approaches have been tested to treat AGU. Limited attempts at bone marrow transplantation (BMT) have not shown any benefit.[3] Enzyme replacement therapy (ERT) has the potential to be an effective treatment, but peripheral administration does not adequately treat the central nervous system (CNS). In addition, manufacture of functional AGA with correct post-translational modifications is technically challenging, leading to significant challenges to implement ERT as a viable clinical treatment.[4,5] Moreover, long-term ERT in a mouse model has been shown to induce immune responses, which abolish its therapeutic effects.[4] More recently, treatment of patient fibroblasts in cell culture with small molecule compounds suggested that these substances may be suitable for AGU as a pharmacological chaperone (PC) mediated therapy,[6,7] and its *in vivo* performance is being tested.

Over the last two decades, there have been numerous viral vector-based gene-therapy (GT) approaches tested for other rare inherited disorders and proved to be clinically therapeutic and safe, in some cases resolving the majority of patients' symptoms.[8] Recombinant adeno-associated viral vector type 9 (AAV9) has particularly been shown to be a safe and efficacious neurotropic vector to deliver transgenes to the CNS.[9] These vectors are non-pathogenic, non-replicating, and transduce both dividing and non-dividing cells. Importantly, they are incapable of coding viral proteins and are primarily non-integrating, making them an ideal vector for gene delivery to the CNS.[10] AAV9 mediates broad gene transfer across the entire

Received 9 June 2020; accepted 3 November 2020;
https://doi.org/10.1016/j.ymthe.2020.11.012.

Correspondence: Steven J. Gray, PhD, Department of Pediatrics, UTSW Medical Center, NA2.508, 6000 Harry Hines Blvd., Dallas, TX 75390, USA.
E-mail: steven.gray@utsouthwestern.edu

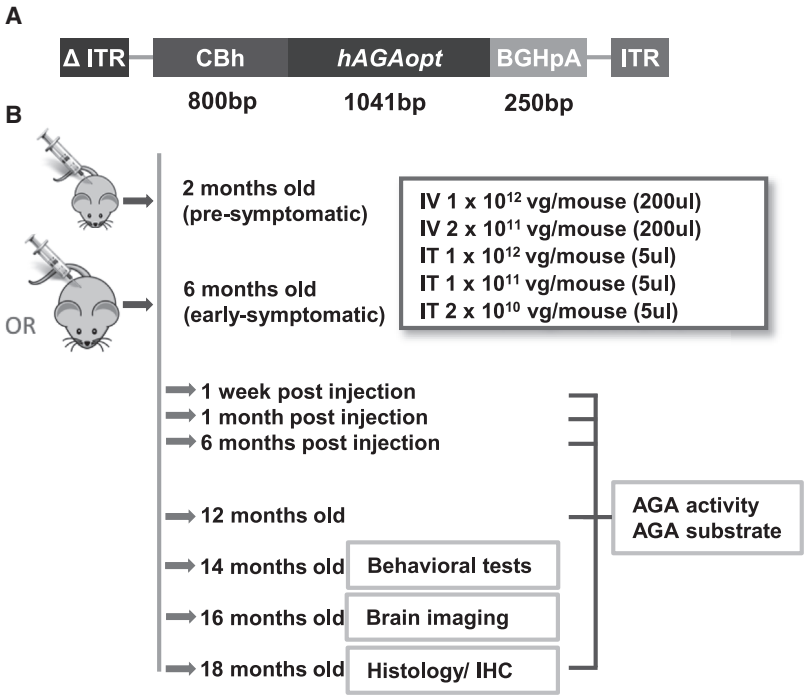

Figure 1. AAV9/*AGA* Vector Construct to Express Human *AGA* and Study Plan of Mouse Experiment

(A) Schematic diagram of the AAV9/*AGA* gene transfer cassette comprising a mutant AAV2 inverted terminal repeat (ITR) with the D element deleted (Δ ITR), the CBh promoter (CMV enhancer, chicken beta actin promoter, synthetic intron), codon-optimized human *AGA* DNA coding sequence (*hAGAopt*), the bovine growth hormone polyadenylation (BGHpA) signal, and WT AAV2 ITR. (B) Study plan, duration, and readouts. Various doses of AAV9/*AGA* vector were administered either intravenously (i.v.) or intrathecally (i.t.) to the mice at 2 months old (pre-symptomatic) or 6 months old (early-symptomatic). Study readouts at each time point after dose administration or at specified age are listed from top to bottom.

CNS in a way that translates from mice to larger animal models.[9–19] Furthermore, AAV9 can be purified in large quantities at high concentrations for potential use in delivering a functional copy of a gene directly to the CNS using either an intravenous (i.v.)[20–22] or intrathecal (i.t.)[9–19] route of administration. The AAV9 vector is being utilized via i.v. administration in the Food and Drug Administration (FDA)-approved GT Zolgensma, for infants with spinal muscular atrophy (SMA). It is also being used in multiple GT clinical trials delivered by an i.t. route, including for giant axonal neuropathy (GAN), SMA, CLN6 Batten disease, and CLN3 Batten disease (ClinicalTrials.gov: NCT02362438, NCT03381729, NCT04273243, and NCT03770572, respectively).

For AGU patients, GT represents a reasonable and promising approach to provide a meaningful and long-term therapeutic benefit for this patient population. AGU is an attractive candidate for GT, as a portion of the expressed enzyme is secreted, and i.v. delivered AGA can be taken up by other cells via the mannose-6-phosphate pathway, potentially treating the condition in non-transduced diseased cell populations.[23] There is also data on restoration of AGA expression in cell lines and animal models supporting an *AGA* GT approach.[24,25]

The $Aga^{-/-}$ mouse model is an accurate genetic model that mirrors the human AGU phenotype for efficacy testing. $Aga^{-/-}$ mice do not have detectable AGA activity, have substrate GlcNAc-Asn accumulation in tissues and body fluids, and exhibit lysosomal hypertrophy in visceral organs, recapitulating the salient features of the human disease.[26–28] By 5 months old, $Aga^{-/-}$ mice have extensive morphoimals were reported to display severe ataxia, and terminally ill animals show extensive gliosis in the brain along with pathological changes in the liver and kidney.

Here, we present preclinical data to support the use of either i.v.- or i.t.-administered AAV9/*AGA* to rescue disease AGU phenotypes in a dose-dependent fashion, either before or after the onset of disease pathology in the $Aga^{-/-}$ mouse model. This AAV9-based GT strategy has the potential to be broadly applied to correct other loss-of-function mutations that lead to CNS disorders.

RESULTS

To test whether we could use AAV9/*AGA* vector construct to rescue the phenotypes in the $Aga^{-/-}$ mice, we created a recombinant AAV9 vector encoding a codon-optimized human *AGA* transgene (h*AGA*opt). The AAV9/*AGA* vector consists of AAV9 capsids that are packaged with the self-complementary (sc) AAV genome comprising a mutant AAV2 inverted terminal repeat (ITR) with the D element deleted (Δ ITR), the CBh promoter (cytomegalovirus [CMV] enhancer, chicken beta actin promoter, and synthetic intron),[31] h*AGA*opt DNA coding sequence, the bovine growth hormone polyadenylation (BGHpA) signal, and wild-type (WT) AAV2 ITR (Figure 1A). The AGA enzyme is highly conserved between human and rodents. The human protein has an 82.37% sequence identity with the mouse protein, with the largest variations found within the signal peptide and the C-terminal propeptide of the α-subunit. These peptides are removed during protein maturation and the sequence of the active enzyme is extremely conserved among species, as is the three-dimensional structure of the AGA enzyme.[32]

To test the safety and efficacy of AAV9/*AGA* vector, we used $Aga^{-/-}$ mice generated and described in 1996 by Kaartinen et al.[26] The mice have a targeted neomycin cassette insertion in exon 3, which leads to premature termination of the polypeptide at amino acid residue 103 and no mRNA transcript. The study plan was as follows, which is outlined in Figure 1B: AAV9/*AGA* was administered to the $Aga^{-/-}$ mice either i.v. with 200 μL of 1×10^{12} or 2×10^{11} vector genome (vg)/

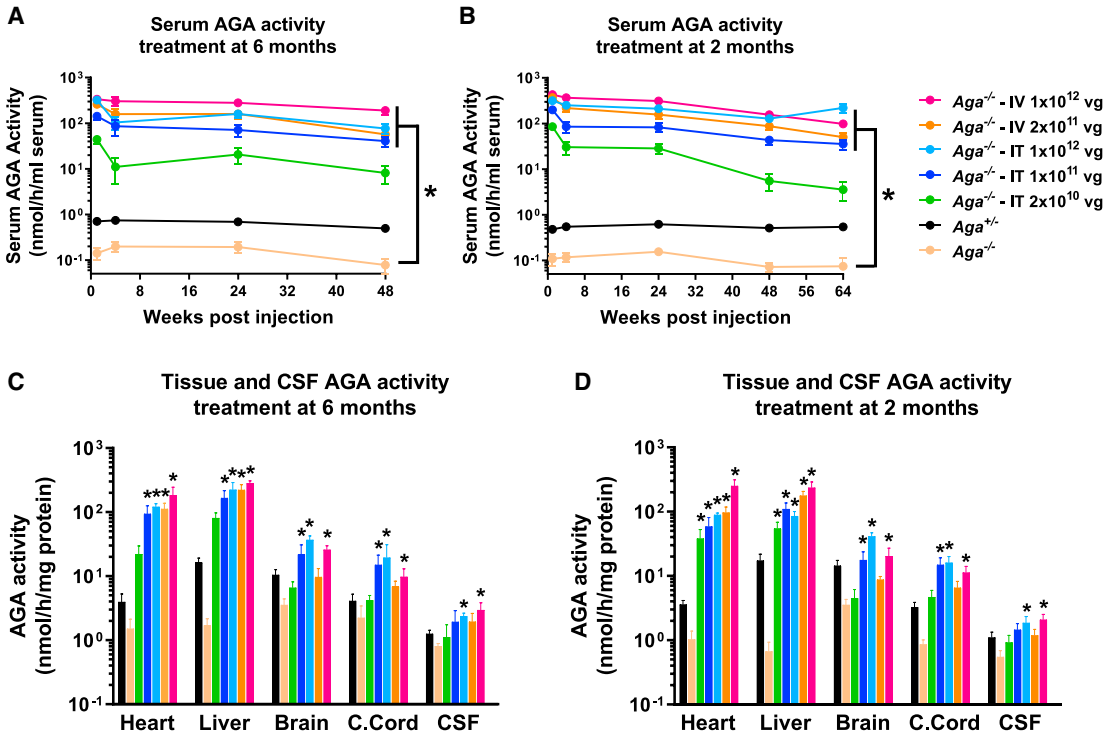

Figure 2. AAV9/*AGA* Gene Therapy (GT) Dose Dependently Increases AGA Activity in Serum, Tissues, and Cerebrospinal Fluid (CSF) to a Supraphysiological Level

(A–D) Various doses of AAV9/*AGA* vector were administered either i.t. or i.v. to $Aga^{-/-}$ mice at 6 months old (A and C) or 2 months old (B and D). AGA activity was assayed in serum sampled at 1, 4, 24, 48 (A and B), and 64 (B) weeks following AAV9/*AGA* administration. AGA activity was assayed in tissue lysates from heart, liver, brain, and cervical spinal cord (c. cord) and in CSF collected at necropsy (C and D) when the mice reached 18 months old. All data are presented as mean ± SEM. * depicts significant difference ($p < 0.05$) by ordinary one-way ANOVA followed by Dunnett's multiple-comparisons test compared to the untreated $Aga^{-/-}$ control. n = 12∼39 in (A), n = 15∼66 in (B), n = 3–6 in (C), and n = 4–8 in (D).

mouse or i.t. with 5 μL of 1×10^{12}, 1×10^{11}, or 2×10^{10} vg/mouse. Cohorts of mice were injected when they were still pre-symptomatic at 2 months old or at 6 months old when they were at early stages of showing AGU-related pathology. AGA activity and AGA substrate GlcNAc-Asn levels were measured in both 2-month and 6-month cohorts at 1 week, 1 month, and 6 months post-injection, and at 12 and 18 months old. Behavioral tests were conducted in all treated animals at 14 months old, and brain imaging was conducted at 16 months old. All remaining mice were sacrificed at 18 months old for histology and immunohistochemistry (IHC) tests.

AAV9/*AGA* GT Increases AGA Activity in $Aga^{-/-}$ Mice

To examine the effects of AAV9/*AGA* vector delivery on levels of AGA protein in mice, serum AGA activity was measured longitudinally following a single dose of AAV9/*AGA* in mice treated at 6 or 2 months old. AGA activity in heterozygous $Aga^{+/-}$ mice is about 40% to 50% that of AGA activity in WT mice, which is sufficient enzyme activity to prevent disease. In the GT-treated $Aga^{-/-}$ mice, AGA activity was increased to supraphysiological levels in a dose-dependent manner in the serum compared to heterozygous carriers (Figures 2A and 2B). At each dose, sustained AGA activity was achieved in the serum over the course of 48 and 64 weeks following the one-dose treatment in 6- or 2-month-old mice (Figures 2A and 2B). AGA activity was also measured in tissue lysates from the heart, liver, brain, and cervical spinal cord, and in cerebral spinal fluid (CSF) collected at necropsy when the mice treated at 6 or 2 months old reached 18 months old. We found a significant dose-dependent increase of AGA activity in different tissues and in CSF to a supraphysiological level (Figures 2C and 2D). We conclude that a one-time delivery of AAV9/*AGA* to $Aga^{-/-}$ mice results in the expression of *AGA* transgene and high levels of AGA enzyme that result in sustained supraphysiological levels of AGA activity.

AAV9/*AGA* GT Reduces AGA Substrate GlcNAc-Asn Accumulation in $Aga^{-/-}$ Mice

Absence of AGA enzymatic activity results in the accumulation of AGA substrate GlcNAc-Asn in the lysosomes of various tissues and body fluids.[33] Large amounts of GlcNAc-Asn substrate can be readily detected in urine of AGU patients and is thereby used as a diagnostic biomarker. GlcNAc-Asn levels were measured longitudinally in the serum and urine at 1, 4, 24, 48, and 64 weeks and in CSF at 18 months old in both mouse cohorts treated with AAV9/*AGA* vector at either 6

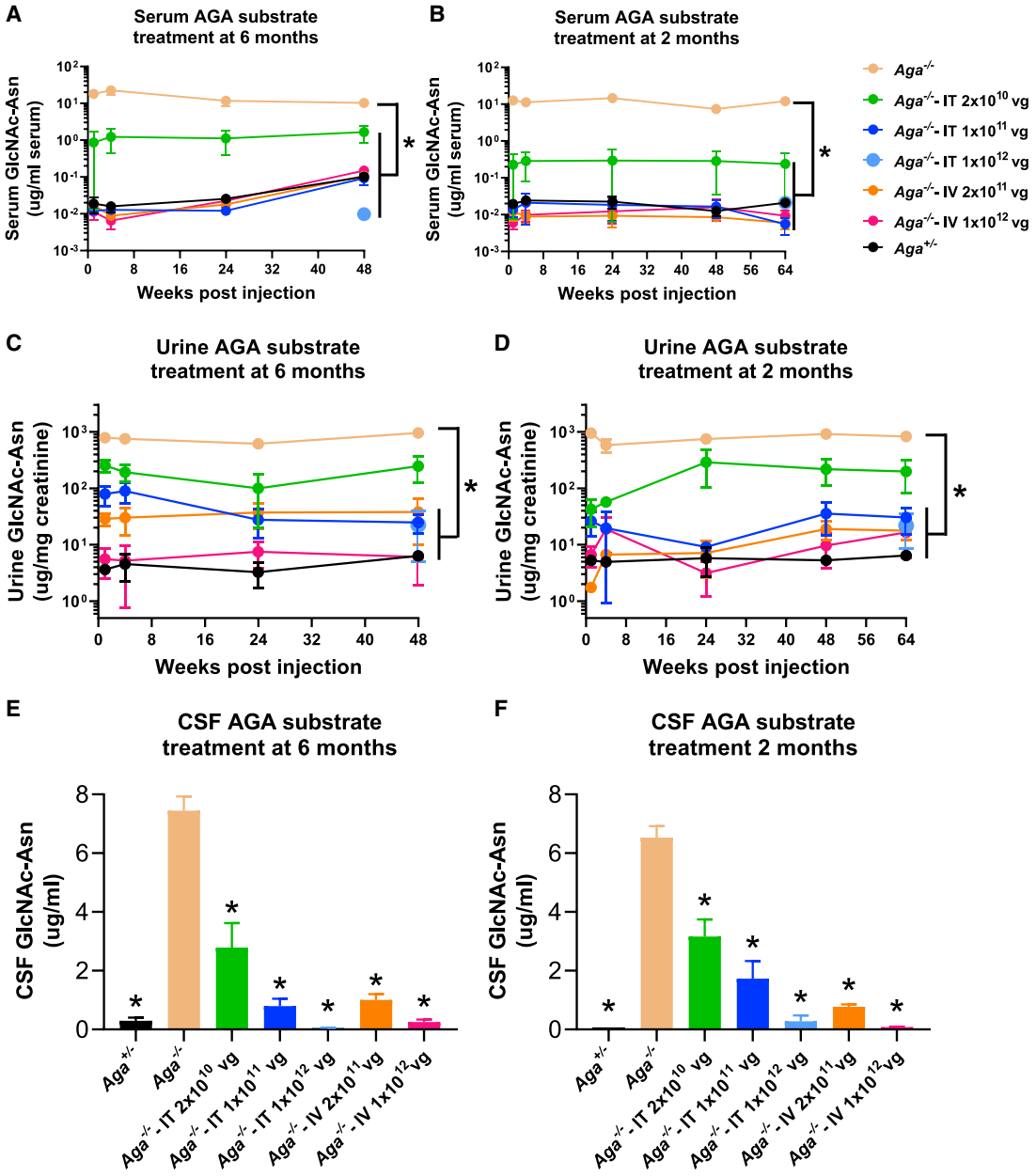

Figure 3. AAV9/*AGA* GT Rapidly and Sustainedly Reduces AGA Substrate Accumulation in Serum, Urine, and CSF

(A–F) Various doses of AAV9/*AGA* vector were administered either i.t. or i.v. to *Aga*$^{-/-}$ mice at 6 months old (A, C, and E) or 2 months old (B, D, and F). AGA substrate was assayed in serum (A and B) and urine (C and D) sampled at 1, 4, 24, 48 (A–D), and 64 (B and D) weeks following AAV9/*AGA* GT. AGA substrate was assayed in CSF (E and F) collected at necropsy when the mice reached 18 months old. All data are presented as mean ± SEM. * depicts significant difference ($p < 0.05$) by ordinary one-way ANOVA followed by Dunnett's multiple-comparisons test compared to the untreated *Aga*$^{-/-}$ control. n = 4–12 in (A), n = 4–10 in (B), n = 4–16 in (C), n = 3–10 in (D), n = 2–14 in (E), and n = 4–14 in (F).

or 2 months old (Figure 3). In the *Aga*$^{-/-}$ mice treated either with an i.v. or i.t. AAV9/*AGA* delivery, serum levels of GlcNAc-Asn were rapidly reduced close to undetectable levels by week 4 post-therapy and maintained at these low levels through week 64 in all treated cohorts except the i.t. low-dose cohort (Figures 3A and B). A similar trend was observed with the urinary excretion of GlcNAc-Asn (Figures 3C and 3D). We also found significant and dose-dependent decreases in the accumulation of GlcNAc-Asn in CSF collected at 18 months old (Figures 3E and 3F). Collectively, compared to control untreated *Aga*$^{-/-}$ mice, mice treated at 6 months or 2 months old i.v.

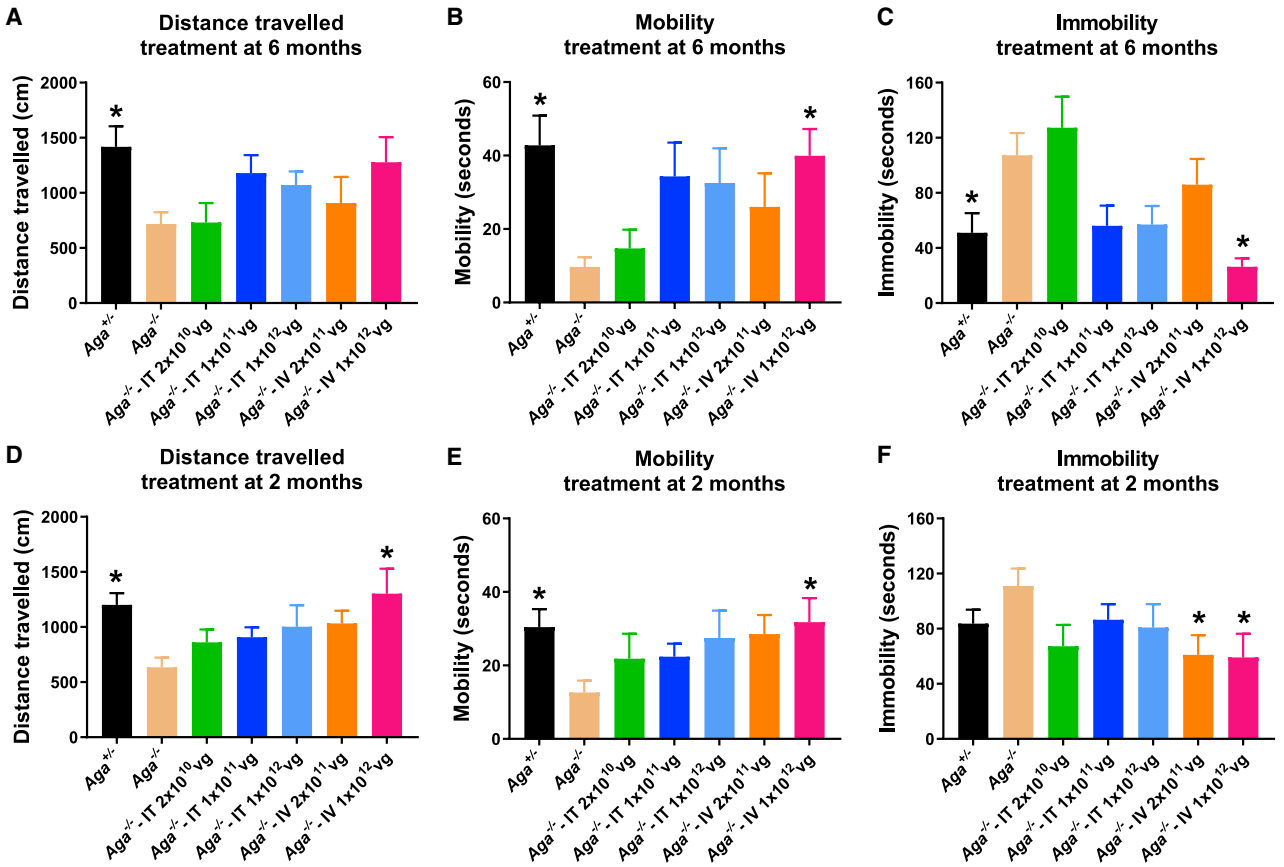

Figure 4. AAV9/*AGA* GT Rescues Abnormal Behavior of *Aga*$^{-/-}$ Mice during the First 5 Min of Open-Field Tests

(A–F) Various doses of AAV9/*AGA* vector were administered either i.t. or i.v. to *Aga*$^{-/-}$ mice at 6 months old (A–C) or 2 months old (D–F). At 14 months old, the mice were allowed to survey an open-field apparatus. The distance traveled in the first 5 min (distance traveled, A and D), time spent highly moving around (mobility, B and E), and time spent still (immobility, C and F) were recorded and quantified by an automated Noldus video tracking system. All data are presented as mean ± SEM. * depicts significant difference ($p < 0.05$) by ordinary one-way ANOVA followed by Dunnett's multiple-comparisons test compared to the untreated *Aga*$^{-/-}$ control. n = 7–21 in (A)–(C), and n = 11–37 in (D)–(F).

or i.t. with high doses of AAV9/*AGA* vector had rapid, sustained, and dose-dependent reductions of the AGA substrate GlcNAc-Asn in the serum, urine, and CSF, to levels similar to those found in the control *Aga*$^{+/-}$ mice.

AAV9/*AGA* GT Rescues Abnormal Behavior of *Aga*$^{-/-}$ Mice during the First 5 Minutes of Open-Field Tests

Based on the progressive nature of AGU, correction of GlcNAc-Asn substrate accumulation is expected to slow or even halt the neurodegeneration, resulting in an amelioration of the phenotypes seen in patients. To test this directly, mice treated at either 6 or 2 months old with AAV9/*AGA* were evaluated at 14 months old, when untreated *Aga*$^{-/-}$ mice show reduced activity in an open-field test. Contrary to previous publication,[26] our colony of AGU mice displayed mild phenotypes overall, with limited tests showing statistically significant differences between *Aga*$^{+/-}$ and *Aga*$^{-/-}$ mice. The open-field test is a tool to assess novel environment exploration, anxiety-related behavior, and general locomotor activity.[34] The mice were allowed to survey an open field, and we measured their distance traveled in the first 5 min as well as time spent with high movement versus time spent still. The first 5 min of the test session was chosen because it sufficiently captures the significant difference of locomotor activity between *Aga*$^{-/-}$ mice and their *Aga*$^{+/-}$ littermates (Figure S1). At 14 months old, *Aga*$^{+/-}$ mice were highly mobile, inspecting the new and unfamiliar surroundings, and spent less time immobile or stationary. In contrast, the untreated *Aga*$^{-/-}$ mice displayed lower exploratory behavior and traveled significantly shorter distances relative to their *Aga*$^{+/-}$ littermates (Figure 4).

Aga$^{-/-}$ mice that received an i.v.- or i.t.-delivered high dose of AAV9/*AGA* had improved activity in open-field tests when compared to the untreated *Aga*$^{-/-}$ mice, irrespective of whether the mice were treated at 6 months (Figures 4A–4C) or at 2 months old (Figures 4D–4F). Both cohorts of mice that had i.v. or i.t. delivery of high-dose AAV9/*AGA* showed a decrease in the time spent still (Figures 4C and 4F), increase in the time spent highly moving around (mobility)

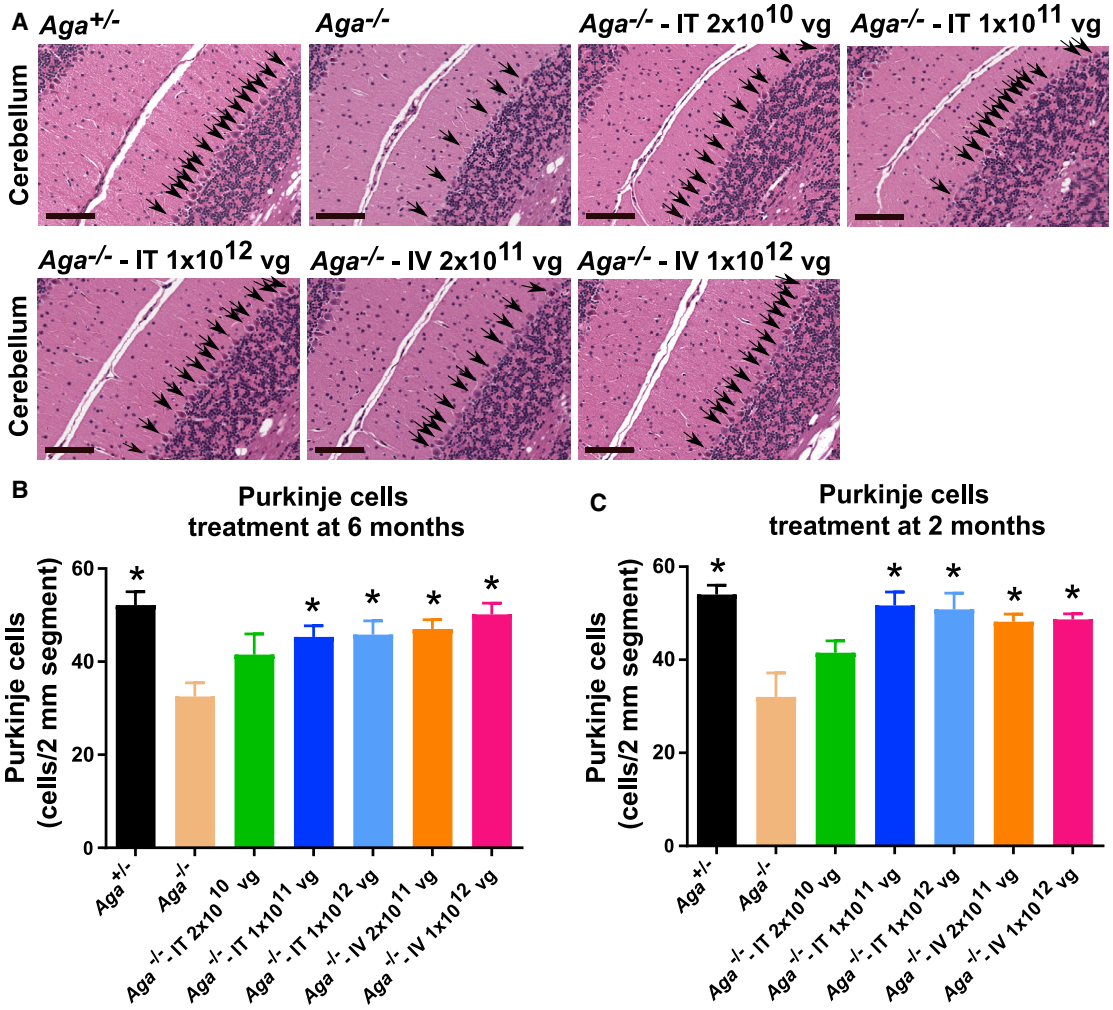

Figure 5. AAV9/*AGA* GT Significantly Preserves Purkinje Cells in the Cerebellum in *Aga*$^{-/-}$ Mice

(A–C) Various doses of AAV9/*AGA* vector were administered either i.t. or i.v. to *Aga*$^{-/-}$ mice treated at 6 months old (A and B) or 2 months old (C). At 18 months old, mouse brain was harvested for hematoxylin and eosin (H&E) staining. Arrows in (A) indicate Purkinje cells, and scale bars in (A) represent 200 μm. All data in (B) and (C) are presented as mean ± SEM. * depicts significant difference ($p < 0.05$) by ordinary one-way ANOVA followed by Dunnett's multiple-comparisons test compared to the untreated *Aga*$^{-/-}$ control. n = 6 in (B), and n = 3–6 in (C).

(Figures 4B and 4E), and increase in distance traveled (Figures 4A and 4D). The i.v. application had a trend toward the strongest corrective effect on these behavioral measures.

AAV9/*AGA* GT Preserves Purkinje Cells in the Cerebellum in *Aga*$^{-/-}$ Mice

Lysosomal hypertrophy as exhibited by cellular vacuolation in visceral organs of the *Aga*$^{-/-}$ mice resembles human AGU histopathology.[28,29] Neuronal, glial, and endothelial cells of the frontal cortex, cerebellum, brain stem, and spinal cord of the AGU mice become vacuolated around 6 months old and progressively worsen. By ten months, *Aga*$^{-/-}$ mice have extensive loss of cerebellar Purkinje neurons, and by > 18 months old ~70%–80% of the Purkinje neurons in the cerebellar cortex are reportedly lost compared to their age-matched *Aga*$^{+/-}$ littermates. We examined the cerebellar histopathology of GT-treated mice compared to their untreated *Aga*$^{-/-}$ controls of the same age (Figure 5A). At 18 months old, hematoxylin and eosin (H&E) staining of cerebellum sections exhibited significant preservation of Purkinje neurons in both cohorts of mice, treated at 6 months or at 2 months old, compared to untreated *Aga*$^{-/-}$ control mice, which exhibited loss of Purkinje neurons in the cerebellum (Figures 5A–5C). These results were further confirmed with IHC staining of Purkinje cells in the cerebellum with an antibody against calbindin (Figure S2). Although we saw a less severe (~40%) loss of Purkinje neurons than what was previously reported (~70%–80% loss) for this *Aga*$^{-/-}$ model, there was significant preservation of these neurons in mice that were treated at 6 months or 2 months old with the two

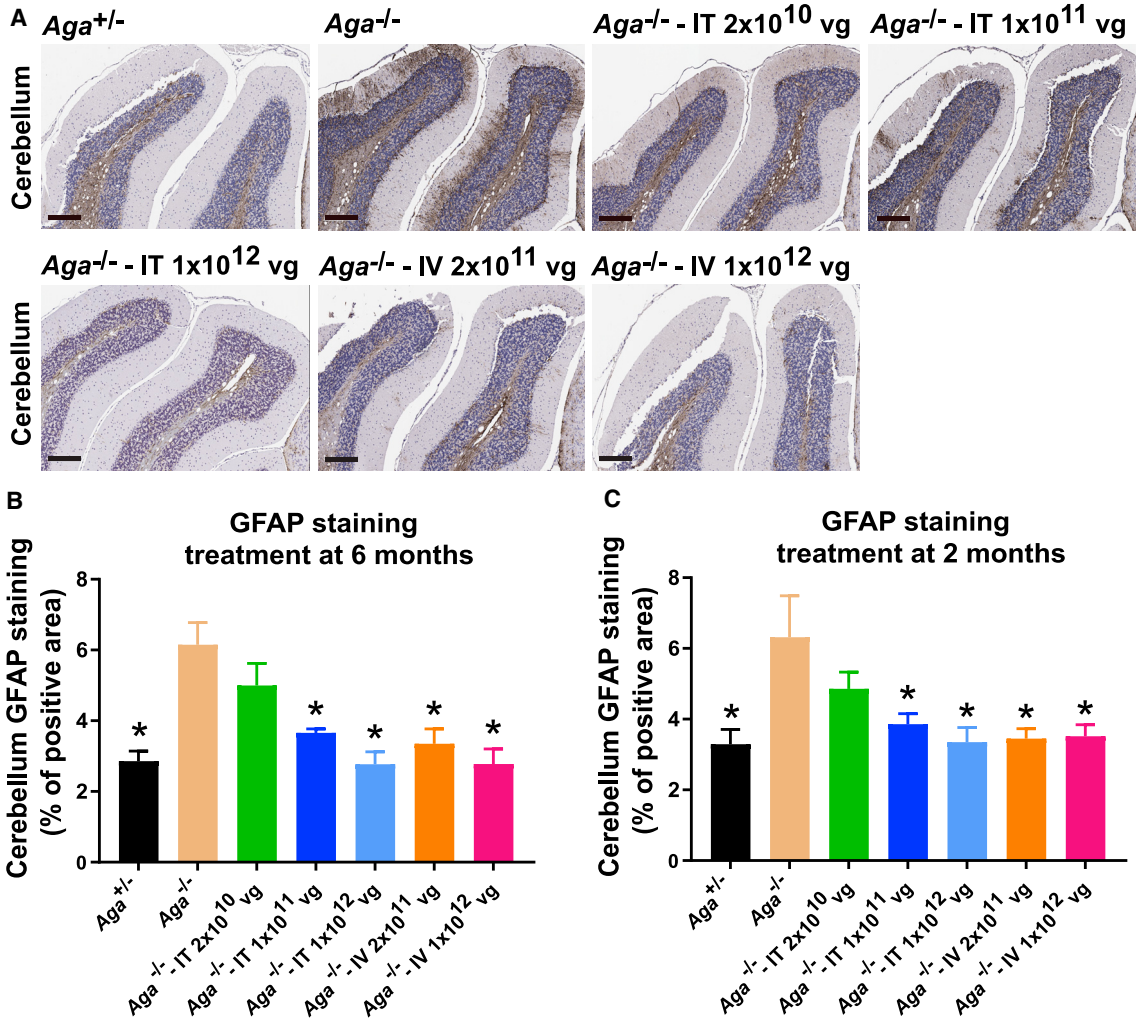

Figure 6. AAV9/*AGA* GT Significantly Reduces Gliosis in *Aga*$^{-/-}$ Mice

(A–C) Various doses of AAV9/*AGA* vector were administered either i.t. or i.v. to *Aga*$^{-/-}$ mice at 6 months old (A and B) or 2 months old (C). At 18 months old, mouse brain was harvested for glial fibrillary acidic protein (GFAP) staining. Scale bars in (A) represent 500 μm. All data in (B) and (C) are presented as mean ± SEM. Asterisk (*) depicts significant difference ($p < 0.05$) by ordinary one-way ANOVA followed by Dunnett's multiple-comparisons test compared to the untreated *Aga*$^{-/-}$ control. n = 6–7 in (B), and n = 7 in (C).

highest i.t. doses and with the low and high i.v. doses (Figures 5B and 5C).

AAV9/*AGA* GT Reduces Gliosis in the CNS in *Aga*$^{-/-}$ Mice

Terminally ill *Aga*$^{-/-}$ mice reportedly show extensive gliosis in the brain.[29] To establish when the onset of gliosis occurs and to what degree in the brains of our *Aga*$^{-/-}$ mice, we initially tested for gliosis at 2 and 6 months old in untreated mice to establish a baseline. Using glial fibrillary acidic protein (GFAP) staining, the 2-month-old *Aga*$^{-/-}$ mice did not have more gliosis in the cerebellum and midbrain compared to their *Aga*$^{+/-}$ littermates (Figures S3B, S3D, and S3E). By 6 months old, the *Aga*$^{-/-}$ mice displayed moderate but not significantly more gliosis in these brain regions compared to their *Aga*$^{+/-}$ littermates (Figures S3A, S3C, and S3E).

We then stained mouse brain for GFAP to evaluate for gliosis[35] after necropsy of the AAV9/*AGA*-treated animals at 18 months old (Figure 6A). Compared to untreated *Aga*$^{-/-}$ control mice, the mice treated at both i.v. doses and the mice treated with the two highest i.t. doses at 6 months or at 2 months old had significantly reduced gliosis, comparable to that seen in the *Aga*$^{+/-}$ control animals (Figures 6B and 6C).

We also assessed GFAP staining within the isocortex, subcortex (hippocampus, thalamus, and hypothalamus), the MPM (midbrain, pons, and medulla), cervical spinal cord, and the lumbar spinal cord to assess for gliosis in these brain regions (Figure S4). Among those animals that received i.v. AAV9/*AGA* at 6 months old, there was a significant decrease in gliosis in the MPM (Figure S4C). Among those

animals that received i.v. AAV9/*AGA* at 2 months old, there was a significant decrease in gliosis in the subcortex and MPM (Figures S4G and S4H). Among the animals that were treated at 2 months old with the highest i.t. dose, there was a significant decrease in gliosis in the subcortex, MPM, and cervical spinal cord (Figures S4G–S4I).

AAV9/*AGA* GT Is Safe and Well-Tolerated in the *Aga*$^{-/-}$ Mice

To assess the safety of the AAV9/*AGA* vector and to ensure there are no non-specific adverse effects on the animal model, brain size and brain weight were assessed in the control *Aga*$^{+/-}$ and *Aga*$^{-/-}$ mice injected with various doses of the AAV9/*AGA* vector, either i.v. or i.t. Sizes of the cerebellum, isocortex, striatum, and ventricle were measured at 16 months old in the animals using magnetic resonance imaging (MRI) (Figures S5A–S5D). There were no significant differences in the sizes of the brain regions between the untreated *Aga*$^{-/-}$, treated *Aga*$^{-/-}$, and *Aga*$^{+/-}$ littermates. Following necropsy at 18 months old, there were also no differences in whole-brain weight (Figure S5E). Additionally, it is worth noting that we were not able to reproduce previously published findings[27,28] of MRI abnormalities in the *Aga*$^{-/-}$ mice.

Injection of AAV9/*AGA* vector with any dose, by either i.v. or i.t. route of delivery, did not reduce survival rate in either the pre-symptomatic or early-symptomatic mice, suggesting the AAV9/*AGA* GT is overall safe and well tolerated (Figure S6). This conclusion is further supported by the histopathological safety report (Supplemental Report) summarized by a blinded licensed veterinary pathologist who concluded that none of the microscopic findings are suggestive of adverse effects related to AAV9/*AGA* vector administration in *Aga*$^{-/-}$ mice.

DISCUSSION

Recombinant AAV9-mediated GT has been extensively used in pre-clinical and clinical studies for the treatment of CNS disorders. Efficacy with AAV9 has been demonstrated in numerous pre-clinical models of CNS disorders and in some clinical studies, using either an i.v. or i.t. route of administration. Here, we tested the feasibility and efficacy of an AAV9-based strategy to deliver the human *AGA* gene to the *Aga*$^{-/-}$ mouse, a model of AGU, an autosomal recessive inherited lysosomal storage disease. Of note, the study was designed as a comprehensive comparison of i.v. and i.t. routes of administration to treat AGU, which could serve as a model for the treatment of other lysosomal storage disorders with similar characteristics as AGU (i.e., CNS pathology and soluble lysosomal enzyme capable of cross-correction).

Apart from the main purpose of the study to evaluate the potential efficacy of AAV9/*AGA*, we also report additional characterization of the mouse model. In general, the phenotype in our colony of *Aga*$^{-/-}$ mice was notably less severe than was previously described.[26,29] Survival was not significantly impacted up to 18 months old, weight was unaffected up to 18 months old, pathology was milder than reported at 6 months and 18 months old, and we did not note the severe morbidity of mice as they approached 18 months old, as originally reported for the model. The caveat to this is that the *Aga*$^{-/-}$ mouse model was on a mixed background (the product of four distinct mouse strain backgrounds), which generated a mouse colony with four different fur colors (silver gray, light brown, dark brown, and black). Although a larger battery of behavioral tests were explored at different ages (rotarod, activity chamber, social novelty, and the Morris water-maze tests, data not shown), the mice generally showed a high degree of variability, and only the open-field test in aged mice was identified as a suitable behavioral outcome. The greatest phenotype affecting morbidity was extreme urinary retention as mice approached 20–21 months of age, which was the primary reason for our predetermined endpoint of 18 months old in our study design. The relatively mild phenotype in mice may be reflective of the protracted disease course in humans. Nevertheless, the mice display key features of the disease and our opinion is that they represent an adequate model to assess treatment efficacy and predict a translational benefit of AAV9/*AGA*.

The *Aga*$^{-/-}$ mice received a single injection of the AAV9/*AGA* before the emergence of disease pathology at 2 months old or at the early stage of disease pathology at 6 months old, in order to test whether the GT could restore AGA function and ameliorate the symptoms associated with AGU. Compared to their *Aga*$^{+/-}$ littermates, AAV9/*AGA* GT increased AGA activity to supraphysiological levels in the *Aga*$^{-/-}$ mice in a dose-dependent manner in serum with pre- and early-symptomatic intervention irrespective of the route of treatment. The activity levels were sustained in the GT-treated *Aga*$^{-/-}$ mice at the last instance of testing, up to 16 months after dosing, confirming stable expression of the human *AGA* transgene and enduring enzyme functionality. High levels of AGA activity detected in the brain tissue indicated efficient AGA enzyme biodistribution to the CNS following GT in the *Aga*$^{-/-}$ mice. The presence of AGA activity in the blood and peripheral tissues of the i.v.- and i.t.-dosed mice indicated that either i.v. or i.t. delivery of AAV9/*AGA* provides functional enzyme throughout the body. Of significance is the high levels of AGA activity in the blood and peripheral tissues following i.t. administration, which is consistent with prior observations that AAV9 distributes to peripheral organs following this route of administration.[11,14,36]

In the treated *Aga*$^{-/-}$ mice, we saw supraphysiological AGA enzyme activity within the CNS and throughout the entire body following GT, either from local expression or cross-correction by circulating enzyme. AGA enzyme activity is a key and relevant biochemical biomarker that is translatable to humans. These increased AGA enzyme levels correlated, in a dose-responsive fashion, with correction of another key translatable biochemical biomarker (AGA substrate GlcNAc-Asn), improved behavioral outcomes (movement in open field), and histopathological improvement (preservation of Purkinje neurons and reduced gliosis). Importantly, the totality of this data converges to an overall conclusion of a comprehensive rescue of the disease at the high dose, achievable via either an i.v. or i.t. route of administration of AAV9/*AGA*.

Although injection of AAV9/*AGA* by either route induces sustained circulating AGA levels that are over 100 times normal, this overabundance of AGA did not create any adverse consequences that we could discern. Compared to their WT littermates, $Aga^{-/-}$ mice are reported to have poor survival, with only 40% surviving past the 20-month mark.[30] In our hands, $Aga^{-/-}$ mice have a median survival rate of over 18 months. There were no signs of morbidity seen in the treatment groups compared to normal $Aga^{+/-}$ mice and untreated $Aga^{-/-}$ mice. There were no differences in weight in treated versus untreated cohorts and no significant differences in survival. Further, treated mice displayed normalized movement patterns rather than any adverse signs. While observations of subtle toxic effects from AAV9/*AGA* are not completely ruled out, our data suggest a favorable long-term safety profile of AAV9/*AGA* at up to one year post-injection.

Both the i.t. and i.v. approaches provided a strong benefit to the $Aga^{-/-}$ mice, and both approaches can translate to humans. A single 1×10^{11} vg i.t. dose provided clear biochemical, histological, and behavioral benefit to $Aga^{-/-}$ mice, as did the higher 1×10^{12} vg i.t. or i.v. dose. A 5-fold lower i.t. dose (2×10^{10} vg) or a 5-fold lower i.v. dose (2×10^{11} vg) resulted in only a partial rescue. The highest 1×10^{12} vg i.t. dose did not provide any further benefit above the 1×10^{11} vg i.t. dose. Thus, our studies set a therapeutic target dose of either 1×10^{11} vg administered i.t. or 1×10^{12} vg (approximately 4×10^{13} vg/kg) administered i.v. Considering that a 10-fold lower dose can be administered i.t. versus i.v. with similar therapeutic effect, our conclusion would be to favor the i.t. route for human translation. Further, the apparent safety of a 10-fold higher (1×10^{12} vg) i.t. dose provides a favorable safety margin.

When considering human translation of the approach, a number of useful points can be derived from this study. First is a target dose, which in mice was 1×10^{11} vg administered i.t. If the dose is scaled by CSF volume, then this would equate to a dose of 4×10^{14} vg total in a human (assuming 0.035 mL of CSF in mice and 140 mL CSF in a human). The CSF volume of humans is relatively static after 3 years old,[37] so this strategy would suggest a target dose of 4×10^{14} vg total in AGU patients > 3 years old, regardless of age. Beyond setting a target dose, our studies characterized two relevant biomarkers that can be measured longitudinally and correlate to a therapeutic response to AAV9/*AGA*: AGA enzyme activity and the AGA enzyme substrate GlcNAc-Asn. AGA enzyme activity can be assessed longitudinally in blood and CSF. AGA enzyme substrate GlcNAc-Asn can be assayed longitudinally in blood, CSF, and urine. Our pre-clinical results predict that both of these biomarkers should respond within weeks of treatment, with AGA enzyme levels elevating to at or above normal levels and AGA enzyme substrate GlcNAc-Asn levels reducing to normal in all 3 body fluids. These $Aga^{-/-}$ studies further predict a behavioral benefit to AGU patients, but extrapolation of the activity in mice (open-field test) to clinical outcomes in humans is clearly less straightforward.

In conclusion, the results achieved in these preclinical studies demonstrate the efficacy and safety of AAV9/*AGA* and strongly support the clinical evaluation in AGU patients, pending the outcomes for further (and more rigorous) pre-clinical safety studies. While either an i.v. or i.t. approach would be predicted to work, we conclude that an i.t. approach should be favored. The conclusions from this study may translate to other AAV9-based gene replacement strategies for related neurological disorders.

MATERIALS AND METHODS

Plasmid Design and Development

We designed and developed the CBh-*hAGAopt*-BGHpA plasmid (Figure 1A) containing the transgene of a human *AGA* codon-optimized construct (*hAGAopt*). The DNA sequence was modified such that the final amino acid sequence is unchanged but there is a significant increase in expression levels of the heterologous gene.[38] The transgene consists of a human *AGA* DNA coding sequence of 1,041 bp between an 800-bp CBh promoter and a 250-bp BGHpA signal. The gene regulatory elements (CBh promoter, BGHpA) are identical to the construct utilized and characterized in these publications, in mice, rats, pigs, and non-human primates.[13,14,20,31] The CBh promoter and BGHpA are utilized for their small size and ability to drive strong expression, allowing for packaging into an scAAV vector.[31]

scAAV9/*AGA* Vector Preparation

Research-grade AAV9/*AGA* vector for pre-clinical testing was manufactured at University of North Carolina Vector Core (UNC-VC). The established plasmid was packaged into sc AAV9 vector,[31] which is 10–100 times more efficient at transduction compared to traditional single-stranded (ss) AAV vectors.[39,40] The final purified product was dialyzed in phosphate-buffered saline (PBS) with an additional 212 mM NaCl and 5% D-sorbitol. Viral titer was determined by qPCR and confirmed by silver stain.[41] The quality control summary of the AAV9/*AGA* vector is included in the Supplemental Information.

$Aga^{-/-}$ Mice

All researches working with mice were approved by the Institutional Animal Care and Use Committee of the University of North Carolina at Chapel Hill (UNC-CH) or the University of Texas Southwestern (UTSW) Medical Center. An $Aga^{-/-}$ mouse was generated and described in 1996 by Kaartinen et al.[26] The mice have a targeted neomycin cassette insertion in exon 3, which leads to premature termination of the polypeptide at amino acid residue 103. The $Aga^{-/-}$ mice do not have a detectable AGA activity and recapitulate the salient features of the human disease.[26,29]

$Aga^{+/-}$ breeders were obtained from Jackson Laboratories. A colony of these mice was established by breeding heterozygous female with homozygous male, and the natural course of the disease was monitored. In general, the disease progression of the colony was slower than was reported by Kaartinen et al.[26] and Gonzalez-Gomez et al.,[29] but the disease was still apparent and consistent with the human phenotype. Mice were identified by toe clipping at post-natal 7 to 10 days and then randomized into treatment groups based on the ID

numbers assigned to them at genotyping. Genotyping was performed using genomic DNA extracted from clipped toe and three primers, AGA-10144 (5′-AGCGTGTGTGTGGTATGCTC-3′), AGA-10145 (5′-TCTGCAAATGCTGTGGTCTC-3′), AGA-Oimr7415 (5′-GCCA GAGGCCACTTGTGTAG-3′). A touchdown protocol with annealing temperature initially from 68°C to 64°C for 7 cycles and then 64°C for 27 cycles more was used for genotyping, which generated a WT band of 361 bp and mutant band of 240 bp.

Mouse Study Plan

The mouse study plan is summarized in Figure 1B. In brief, both male and female *Aga*$^{-/-}$ mice were injected either i.v. or i.t. at 2 months old (pre-symptomatic cohorts) or 6 months old (early-symptomatic cohorts). For i.v. administration, 200 μL of either a high (1×10^{12} vg/mouse) or low (2×10^{11} vg/mouse) dose of scAAV9/*AGA* vector was administrated via tail vein. For i.t., 5 μL of either a very high (1×10^{12} vg/mouse), high (1×10^{11} vg/mouse), or low (2×10^{10} vg/mouse) dose of scAAV9/*AGA* vector was administrated via lumber puncture. Injection volumes and vehicle composition was held constant across all dose levels. Serum and urine were collected for the measurement of AGA activity and AGA substrate at different time points post-injection. Behavioral tests and brain imaging were performed at 14 or 16 months old, respectively. Necropsy, histopathology, and toxicity evaluation were performed at the end of the experiment when mice reached 18 months old. *Aga*$^{+/-}$ mice were phenotypically normal, and age/sex-matched littermates were used as normal controls.

AGA Activity Assay

AGA activity assay was conducted using the method described previously[33] with some modification. To measure serum AGA activity, 5 μL of each mouse serum was mixed with 20 μL of substrate buffer (pH 6.5) containing 1 mM of L-aspartic acid-β-7-amido-4-methylcoumarin (A1057-50 mg, Sigma-Aldrich) and 5 μL of reaction buffer containing 1× Hank's balanced salt solution (HBSS) and 10 mM HEPES. This reaction was incubated at 37°C and 200 rpm for 1 h for samples from treated mice or 24 h for samples from untreated mice. The serum AGA activity was calculated against a standard curve and expressed as nmol/h/mL serum. To measure tissue AGA activity, approximately 25 mg of heart, liver, brain, or cervical spinal cord were mixed with 400 μL of deionized water and a 4.5-mm steel bead and physically lysed for 5 min at a speed of 25/s with a Tissuelyzer. After a freeze at −80°C overnight and thaw at room temperature, the samples were lysed again the same way and then centrifuged 3,000 × *g* at 4°C for 10 min. Tissue AGA activity was measured using 5 μL of supernatant of each sample. CSF AGA activity was measured using 2.5 μL of CSF. The AGA activity from both tissue and CSF was normalized against their respective protein concentration and expressed as nmol/h/mg protein.

AGA Substrate Assay

Analysis of the AGA substrate was conducted at Greenwood Genetics Center in a blinded fashion using coded samples. 15 μL of each sample, 3 μL of AGU internal standard (50 μg/mL), and 132 μL of 90% acetonitrile were added into one 1.5-mL centrifuge tube and vortexed immediately. Following the centrifugation at 13,000 rpm for 5 min, all supernatant was transferred into a 0.22-μm filter spin tube and centrifuged at 13,000 rpm for 1 min. The filtrate was then transferred from the filter tube to the polyspring insert in a wide-mouth screw cap vial and capped with a split liner.

Ultraperformance liquid chromatography (UPLC) separation utilized an Acquity I-class system equipped with a UPLC glycan BEH amide column (1.7 μm, 2.1 mm × 50 mm) with a VanGuard glycan BEH amide 1.7 μm guard column (5 × 2.1 mm, 1.7 μm), all from Waters. Analytes were separated utilizing an elution gradient with water with 50 mM ammonium formate at pH 4.5 (mobile phase A) and acetonitrile (mobile phase B), a column temperature of 60°C, and a flow rate of 0.5 mL/min. A triple-quadrupole tandem mass spectrometer (Xevo TQ-S; Waters) was used in positive-ion detection mode. The tandem mass spectrometry (MS/MS) transition for the analytes was 336.14 > 204.05 and for the internal standard was 339.14 > 207.05. The capillary voltage was 2 kV, the cone voltage was 40 V, and the collision energy was 10 eV. The source temperature was 120°C, and the desolvation temperature was 60°C.

Open-Field Test

The open-field test consisted of an arena that was a 40 cm × 40 cm × 30 cm (L × W × H) plastic apparatus. The central square 20-cm × 20-cm region was designated as the central area, and the rest of the open field was considered as peripheral area.[42] Mice were habituated to the experimental room for more than ten minutes prior to testing and then placed in the center of the arena at the beginning of the test period. As soon as the experimenter is out of view of the camera the testing period begins and last for 5 min. The apparatus was sprayed with 70% ethanol between each mouse, dried with paper towels, and left to air dry for 5 min. The video-tracking software Ethovision 12 (Noldus Information Technologies; Wageningen, the Netherlands) was used to measure the following parameters: total distance traveled, duration of mobility, and duration of immobility.

H&E and IHC Staining

Mouse tissues were drop fixed for 3 days in 10% phosphate-buffered formalin following perfusion of the mouse with PBS containing 1 U/mL heparin and transferred into 70% ethanol. Mouse brain, cervical spinal cord, and lumber spinal cord were paraffin processed, embedded, and cut into 5-μm sections either for H&E or IHC staining. For IHC, the sections were treated with antigen retrieval solution (H3300, Vector Laboratories) and then with 3% hydrogen peroxide (H_2O_2) to remove endogenous peroxidase activity. After incubation for 1 h at room temperature in blocking buffer containing 5% goat serum and avidin solution (SP2001, Vector Laboratories) in 1× PBS, the sections were incubated overnight at 4°C in primary antibody solution containing 5% goat serum and 1:4,000 rabbit anti-GFAP antibody (Z0334, Dako) or 1:200 rabbit anti-calbindin antibody (2173S, Cell Signaling) in 1× PBS and then incubated for 1 h at room temperature in second antibody solution containing 5% goat serum and 1:200 biotinylated anti-rabbit immunoglobulin

G (IgG) (BA-1000, Vector Laboratories) in 1× PBS. Color development was performed with a Vectstain ABC kit (PK-6100, Vector Laboratories) with 3,3′-diaminobenzidine tetrachloride (DAB) (TA-125-QHDX, Thermo Scientific) substrate and counterstaining with modified Mayer's hemotoxylin (72804, Richard-Allan Scientific). All stained slides were digitized with a ScanScope slide scanner (Aperio Technologies), and scanned slides were viewed with ImageScope software package (version 10.0; Aperio Technologies). GFAP staining intensity was quantified with Halo software package (Halo2.2; Indica Labs).

MRI

T2 weighted images were acquired with a 3D RARE sequence on a Bruker 9.4 T animal MRI scanner. The sequence parameters are as follows: TR = 3000 ms, TE = 56 ms, RARE factor = 8, matrix size 133 × 96 × 96, voxel size = 0.15 × 0.15 × 0.15 mm^3, and total duration = 39.06 min. During the scan, the animals were anesthetized by inhaling ∼2% isoflurane and oxygen mixture through a nose cone. They were placed on a custom-made cradle in a prone position, and their heads were fixed using tooth and ear bars. Body temperature and respiratory rate were continuously monitored and maintained within normal ranges over the duration of the scan (37 ± 0.5 °C, 80 ± 20 bpm, respectively). The T2 weighted images were segmented using a fully automated rodent brain MR image processing pipeline.[43] Based on the segmentation masks, the volumes of the cerebellum, isocortex, striatum, and ventricle were calculated and compared between the six groups. Operators and image analyzers were blind to genotype and treatment, which was conducted by the Animal MRI (CAMRI) and Biomedical Research Imaging Center (BRIC) at UNC.

Statistical Analysis

All data in this paper were presented as mean ± SEM, analyzed, and graphed using GraphPad Prism software (version 7.04, GraphPad Software). Student's unpaired t test was used for two-group comparison and one-way ANOVA followed by Dunnett's multiple comparisons test compared to the untreated $AGA^{-/-}$ control was used for equal or more-than-three-group comparison. Statistical significance was set as $p < 0.05$.

SUPPLEMENTAL INFORMATION

Supplemental Information can be found online at https://doi.org/10.1016/j.ymthe.2020.11.012.

ACKNOWLEDGMENTS

This study was supported by the Rare Trait Hope Fund (USA), the UNC TraCS Institute(USA, 550KR121511), and AFM-Téléthon (France, Award 19715) to S.J.G. We thank Jackson Laboratories for providing the $AGA^{+/-}$ breeders, the UNC Vector Core facility for producing some vectors used in these studies, and Greenwood Genetics Center for performing the AGA substrate assays. We thank the members at the UNC Center for Animal MRI (CAMRI) and Biomedical Research Imaging Center (BRIC) for technical assistance, supported in part by the Bowles Center for Alcohol Studies (P60 AA011605), the Lineberger Comprehensive Center (P30 CA016086), and the Carolina Institute for Developmental Disabilities (U54 HD079124). We also acknowledge Dr. Thomas Dong for his help in sample preparation, Dr. Mary Wight-Carter for her toxicity evaluation and histopathological safety report, Dr. Anna Azvolinsky for her support in manuscript preparation, and Dr. Stuart Cobb for his insightful manuscript review.

AUTHOR CONTRIBUTIONS

X.C. and S.J.G. designed the experiments, coordinated studies with collaborators and core facilities, and wrote the manuscript. X.C., S.S.-V., L.P., and Y.H. performed the experiments. S.S.C. served as a consultant on this project. X.C. analyzed all data and prepared all figures for the manuscript. L.P. and Y.H. helped writing the Materials and Methods section. R.T. advised the project, shared protocols, and reviewed the manuscript. S.J.G. oversaw all activities related to the project and acquired all funding for the work.

DECLARATION OF INTERESTS

S.J.G. has received patent royalties for intellectual property (IP) licensed to Asklepios Biophama, but this IP was not used in this study. S.J.G. is an inventor of the AGA vector design and has received patent royalties on this technology from Neurogene.

REFERENCES

1. Arvio, M., and Mononen, I. (2016). Aspartylglycosaminuria: a review. Orphanet J. Rare Dis. *11*, 162.
2. Arvio, P., and Arvio, M. (2002). Progressive nature of aspartylglucosaminuria. Acta Paediatr. *91*, 255–257.
3. Arvio, M., Sauna-Aho, O., and Peippo, M. (2001). Bone marrow transplantation for aspartylglucosaminuria: follow-up study of transplanted and non-transplanted patients. J. Pediatr. *138*, 288–290.
4. Dunder, U., Kaartinen, V., Valtonen, P., Väänänen, E., Kosma, V.M., Heisterkamp, N., Groffen, J., and Mononen, I. (2000). Enzyme replacement therapy in a mouse model of aspartylglycosaminuria. FASEB J. *14*, 361–367.
5. Dunder, U., Valtonen, P., Kelo, E., and Mononen, I. (2010). Early initiation of enzyme replacement therapy improves metabolic correction in the brain tissue of aspartylglycosaminuria mice. J. Inherit. Metab. Dis. *33*, 611–617.
6. Banning, A., Gülec, C., Rouvinen, J., Gray, S.J., and Tikkanen, R. (2016). Identification of small molecule compounds for pharmacological chaperone therapy of aspartylglucosaminuria. Sci. Rep. *6*, 37583.
7. Banning, A., Schiff, M., and Tikkanen, R. (2018). Amlexanox provides a potential therapy for nonsense mutations in the lysosomal storage disorder Aspartylglucosaminuria. Biochim. Biophys. Acta Mol. Basis Dis. *1864*, 668–675.
8. Naldini, L. (2015). Gene therapy returns to centre stage. Nature *526*, 351–360.
9. Saraiva, J., Nobre, R.J., and Pereira de Almeida, L. (2016). Gene therapy for the CNS using AAVs: The impact of systemic delivery by AAV9. J. Control. Release *241*, 94–109.
10. Choudhury, S.R., Hudry, E., Maguire, C.A., Sena-Esteves, M., Breakefield, X.O., and Grandi, P. (2017). Viral vectors for therapy of neurologic diseases. Neuropharmacology *120*, 63–80.
11. Bailey, R.M., Armao, D., Nagabhushan Kalburgi, S., and Gray, S.J. (2018). Development of intrathecal AAV9 gene therapy for giant axonal neuropathy. Mol. Ther. Methods Clin. Dev. *9*, 160–171.
12. Karumuthil-Melethil, S., Marshall, M.S., Heindel, C., Jakubauskas, B., Bongarzone, E.R., and Gray, S.J. (2016). Intrathecal administration of AAV/GALC vectors in 10-11-day-old twitcher mice improves survival and is enhanced by bone marrow transplant. J. Neurosci. Res. *94*, 1138–1151.

13. Federici, T., Taub, J.S., Baum, G.R., Gray, S.J., Grieger, J.C., Matthews, K.A., Handy, C.R., Passini, M.A., Samulski, R.J., and Boulis, N.M. (2012). Robust spinal motor neuron transduction following intrathecal delivery of AAV9 in pigs. Gene Ther. *19*, 852–859.

14. Gray, S.J., Nagabhushan Kalburgi, S., McCown, T.J., and Jude Samulski, R. (2013). Global CNS gene delivery and evasion of anti-AAV-neutralizing antibodies by intrathecal AAV administration in non-human primates. Gene Ther. *20*, 450–459.

15. Snyder, B.R., Gray, S.J., Quach, E.T., Huang, J.W., Leung, C.H., Samulski, R.J., Boulis, N.M., and Federici, T. (2011). Comparison of adeno-associated viral vector serotypes for spinal cord and motor neuron gene delivery. Hum. Gene Ther. *22*, 1129–1135.

16. Masamizu, Y., Okada, T., Kawasaki, K., Ishibashi, H., Yuasa, S., Takeda, S., Hasegawa, I., and Nakahara, K. (2011). Local and retrograde gene transfer into primate neuronal pathways via adeno-associated virus serotype 8 and 9. Neuroscience *193*, 249–258.

17. Bucher, T., Colle, M.A., Wakeling, E., Dubreil, L., Fyfe, J., Briot-Nivard, D., Maquigneau, M., Raoul, S., Cherel, Y., Astord, S., et al. (2013). scAAV9 intracisternal delivery results in efficient gene transfer to the central nervous system of a feline model of motor neuron disease. Hum. Gene Ther. *24*, 670–682.

18. Haurigot, V., Marcó, S., Ribera, A., Garcia, M., Ruzo, A., Villacampa, P., Ayuso, E., Añor, S., Andaluz, A., Pineda, M., et al. (2013). Whole body correction of mucopolysaccharidosis IIIA by intracerebrospinal fluid gene therapy. J. Clin. Invest. *123*, 3254–3271.

19. Samaranch, L., Salegio, E.A., San Sebastian, W., Kells, A.P., Bringas, J.R., Forsayeth, J., and Bankiewicz, K.S. (2013). Strong cortical and spinal cord transduction after AAV7 and AAV9 delivery into the cerebrospinal fluid of nonhuman primates. Hum. Gene Ther. *24*, 526–532.

20. Gray, S.J., Matagne, V., Bachaboina, L., Yadav, S., Ojeda, S.R., and Samulski, R.J. (2011). Preclinical differences of intravascular AAV9 delivery to neurons and glia: a comparative study of adult mice and nonhuman primates. Mol. Ther. *19*, 1058–1069.

21. Duque, S., Joussemet, B., Riviere, C., Marais, T., Dubreil, L., Douar, A.M., Fyfe, J., Moullier, P., Colle, M.A., and Barkats, M. (2009). Intravenous administration of self-complementary AAV9 enables transgene delivery to adult motor neurons. Mol. Ther. *17*, 1187–1196.

22. Foust, K.D., Nurre, E., Montgomery, C.L., Hernandez, A., Chan, C.M., and Kaspar, B.K. (2009). Intravascular AAV9 preferentially targets neonatal neurons and adult astrocytes. Nat. Biotechnol. *27*, 59–65.

23. Sands, M.S., and Davidson, B.L. (2006). Gene therapy for lysosomal storage diseases. Mol. Ther. *13*, 839–849.

24. Peltola, M., Kyttälä, A., Heinonen, O., Rapola, J., Paunio, T., Revah, F., Peltonen, L., and Jalanko, A. (1998). Adenovirus-mediated gene transfer results in decreased lysosomal storage in brain and total correction in liver of aspartylglucosaminuria (AGU) mouse. Gene Ther. *5*, 1314–1321.

25. Harkke, S., Laine, M., and Jalanko, A. (2003). Aspartylglucosaminidase (AGA) is efficiently produced and endocytosed by glial cells: implication for the therapy of a lysosomal storage disorder. J. Gene Med. *5*, 472–482.

26. Kaartinen, V., Mononen, I., Voncken, J.W., Noronkoski, T., Gonzalez-Gomez, I., Heisterkamp, N., and Groffen, J. (1996). A mouse model for the human lysosomal disease aspartylglycosaminuria. Nat. Med. *2*, 1375–1378.

27. Jalanko, A., Tenhunen, K., McKinney, C.E., LaMarca, M.E., Rapola, J., Autti, T., Joensuu, R., Manninen, T., Sipilä, I., Ikonen, S., et al. (1998). Mice with an aspartylglucosaminuria mutation similar to humans replicate the pathophysiology in patients. Hum. Mol. Genet. *7*, 265–272.

28. Tenhunen, K., Uusitalo, A., Autti, T., Joensuu, R., Kettunen, M., Kauppinen, R.A., Ikonen, S., LaMarca, M.E., Haltia, M., Ginns, E.I., et al. (1998). Monitoring the CNS pathology in aspartylglucosaminuria mice. J. Neuropathol. Exp. Neurol. *57*, 1154–1163.

29. Gonzalez-Gomez, I., Mononen, I., Heisterkamp, N., Groffen, J., and Kaartinen, V. (1998). Progressive neurodegeneration in aspartylglycosaminuria mice. Am. J. Pathol. *153*, 1293–1300.

30. Kaartinen, V., Mononen, I., Gonzalez-Gomez, I., Noronkoski, T., Heisterkamp, N., and Groffen, J. (1998). Phenotypic characterization of mice with targeted disruption of glycosylasparaginase gene: a mouse model for aspartylglycosaminuria. J. Inherit. Metab. Dis. *21*, 207–209.

31. Gray, S.J., Foti, S.B., Schwartz, J.W., Bachaboina, L., Taylor-Blake, B., Coleman, J., Ehlers, M.D., Zylka, M.J., McCown, T.J., and Samulski, R.J. (2011). Optimizing promoters for recombinant adeno-associated virus-mediated gene expression in the peripheral and central nervous system using self-complementary vectors. Hum. Gene Ther. *22*, 1143–1153.

32. Tikkanen, R., Peltola, M., Oinonen, C., Rouvinen, J., and Peltonen, L. (1997). Several cooperating binding sites mediate the interaction of a lysosomal enzyme with phosphotransferase. EMBO J. *16*, 6684–6693.

33. Mononen, I.T., Kaartinen, V.M., and Williams, J.C. (1993). A fluorometric assay for glycosylasparaginase activity and detection of aspartylglycosaminuria. Anal. Biochem. *208*, 372–374.

34. Prut, L., and Belzung, C. (2003). The open field as a paradigm to measure the effects of drugs on anxiety-like behaviors: a review. Eur. J. Pharmacol. *463*, 3–33.

35. Yang, Z., and Wang, K.K. (2015). Glial fibrillary acidic protein: from intermediate filament assembly and gliosis to neurobiomarker. Trends Neurosci. *38*, 364–374.

36. Sinnett, S.E., Hector, R.D., Gadalla, K.K.E., Heindel, C., Chen, D., Zaric, V., Bailey, M.E.S., Cobb, S.R., and Gray, S.J. (2017). Improved MECP2 gene therapy extends the survival of MeCP2-null mice without apparent toxicity after intracisternal delivery. Mol. Ther. Methods Clin. Dev. *5*, 106–115.

37. Bleyer, W.A., and Dedrick, R.L. (1977). Clinical pharmacology of intrathecal methotrexate. I. Pharmacokinetics in nontoxic patients after lumbar injection. Cancer Treat. Rep. *61*, 703–708.

38. Banning, A., König, J.F., Gray, S.J., and Tikkanen, R. (2017). Functional analysis of the Ser149/Thr149 variants of human aspartylglucosaminidase and optimization of the coding sequence for protein production. Int. J. Mol. Sci. *18*, 706–718.

39. McCarty, D.M., Fu, H., Monahan, P.E., Toulson, C.E., Naik, P., and Samulski, R.J. (2003). Adeno-associated virus terminal repeat (TR) mutant generates self-complementary vectors to overcome the rate-limiting step to transduction in vivo. Gene Ther. *10*, 2112–2118.

40. McCarty, D.M., Monahan, P.E., and Samulski, R.J. (2001). Self-complementary recombinant adeno-associated virus (scAAV) vectors promote efficient transduction independently of DNA synthesis. Gene Ther. *8*, 1248–1254.

41. Gray, S.J., Choi, V.W., Asokan, A., Haberman, R.A., McCown, T.J., and Samulski, R.J. (2011). Production of recombinant adeno-associated viral vectors and use in in vitro and in vivo administration. Curr. Protoc. Neurosci. *57*, 4.17.1–4.17.30.

42. Christakis, D.A., Ramirez, J.S., and Ramirez, J.M. (2012). Overstimulation of newborn mice leads to behavioral differences and deficits in cognitive performance. Sci. Rep. *2*, 546.

43. Budin, F., Hoogstoel, M., Reynolds, P., Grauer, M., O'Leary-Moore, S.K., and Oguz, I. (2013). Fully automated rodent brain MR image processing pipeline on a Midas server: from acquired images to region-based statistics. Front. Neuroinform. *7*, 15.

YMTHE, Volume *29*

Supplemental Information

Pre-clinical Gene Therapy with AAV9/*AGA* in Aspartylglucosaminuria Mice Provides Evidence for Clinical Translation

Xin Chen, Sarah Snanoudj-Verber, Laura Pollard, Yuhui Hu, Sara S. Cathey, Ritva Tikkanen, and Steven J. Gray

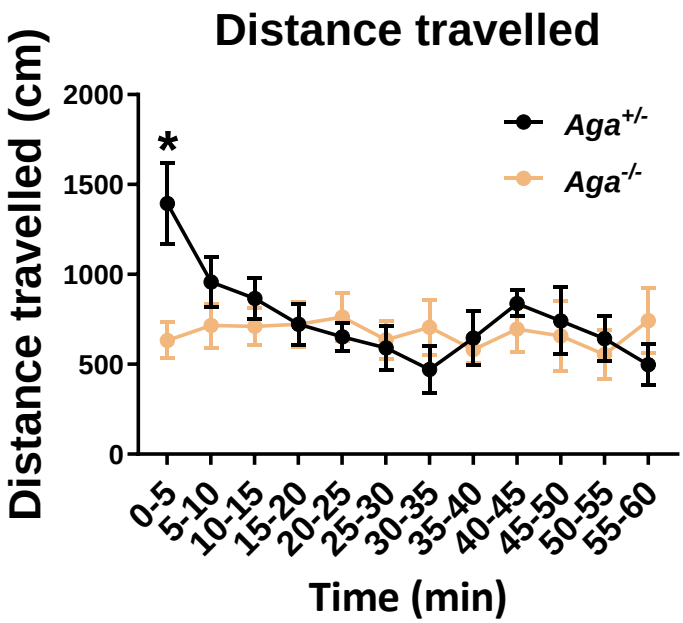

Supplemental Figure 1. *Aga*$^{-/-}$ mice at 14 months old travels significantly shorter distance during the first 5-minutes of open field tests than their *Aga*$^{+/-}$ littermates. Open field tests were performed on mice (n=12) when they reached 14 months old and distance travelled was calculated. All data are presented as mean ± SEM. * depicts significant difference ($p<0.05$) by unpaired t-test compared to the untreated *Aga*$^{-/-}$ control.

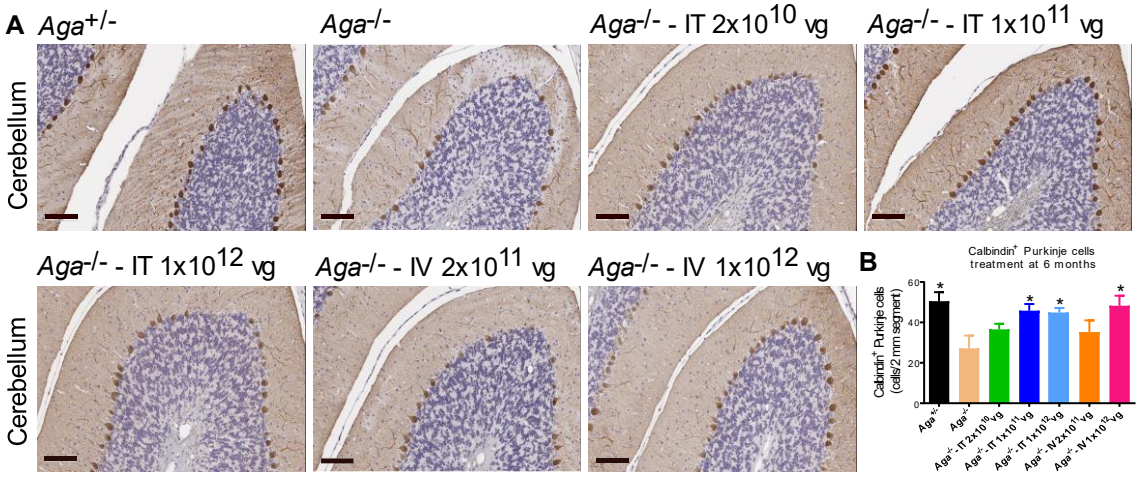

Supplemental Figure 2. AAV9/*AGA* GT significantly preserves Calbindin+ Purkinje cells in the cerebellum in *Aga*. Various doses of AAV9/*AGA* vector were administered either IT or IV to *Aga*$^{-/-}$ mice treated at 6 months old. At 18 months old, mouse brain was harvested for IHC staining using an antibody against Calbindin. Scale bars in panel A represent 100 µm. Data in panel B are presented as mean±SEM. *depicts significant difference ($p<0.05$) by ordinary one-way ANOVA followed by Dunnett's multiple comparisons test compared to the untreated *Aga*$^{-/-}$ control. n=5-6 in (B).

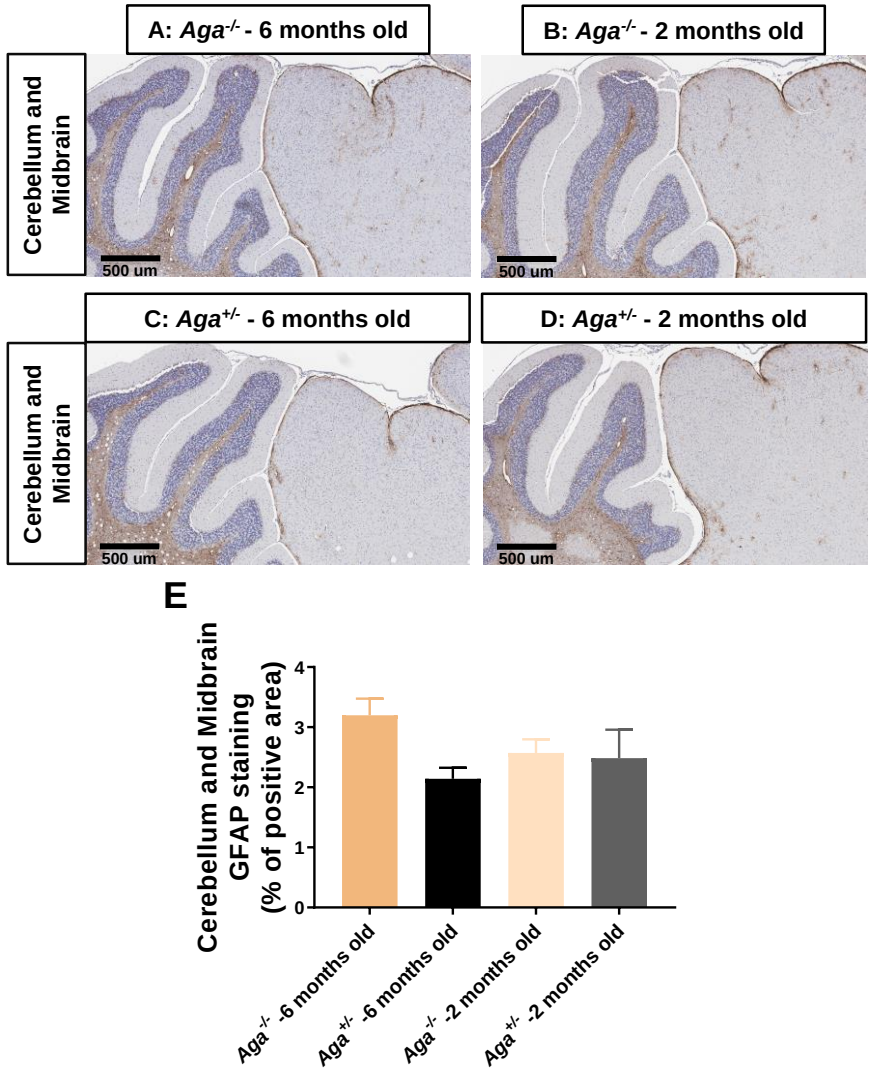

Supplemental Figure 3. *Aga*$^{-/-}$ mouse at 6 months old (A), but not at 2 months old (B), shows moderate but not significantly more gliosis than its *Aga*$^{+/-}$ littermates (C, D, and E). Mouse brain was harvested at 6 months old (**A and C**) or 2 months old (**B and D**) for glial fibrillary acidic protein (GFAP) staining. Significant difference were analyzed by ordinary one-way ANOVA followed by Dunnett's multiple comparisons test compared to the untreated *Aga*$^{-/-}$ control. No significant differences were found between any cohorts. Scale bars in all panels (**A-D**) represent 500 µm. All data in panel **E** (n=3-6) are presented as mean ± SEM.

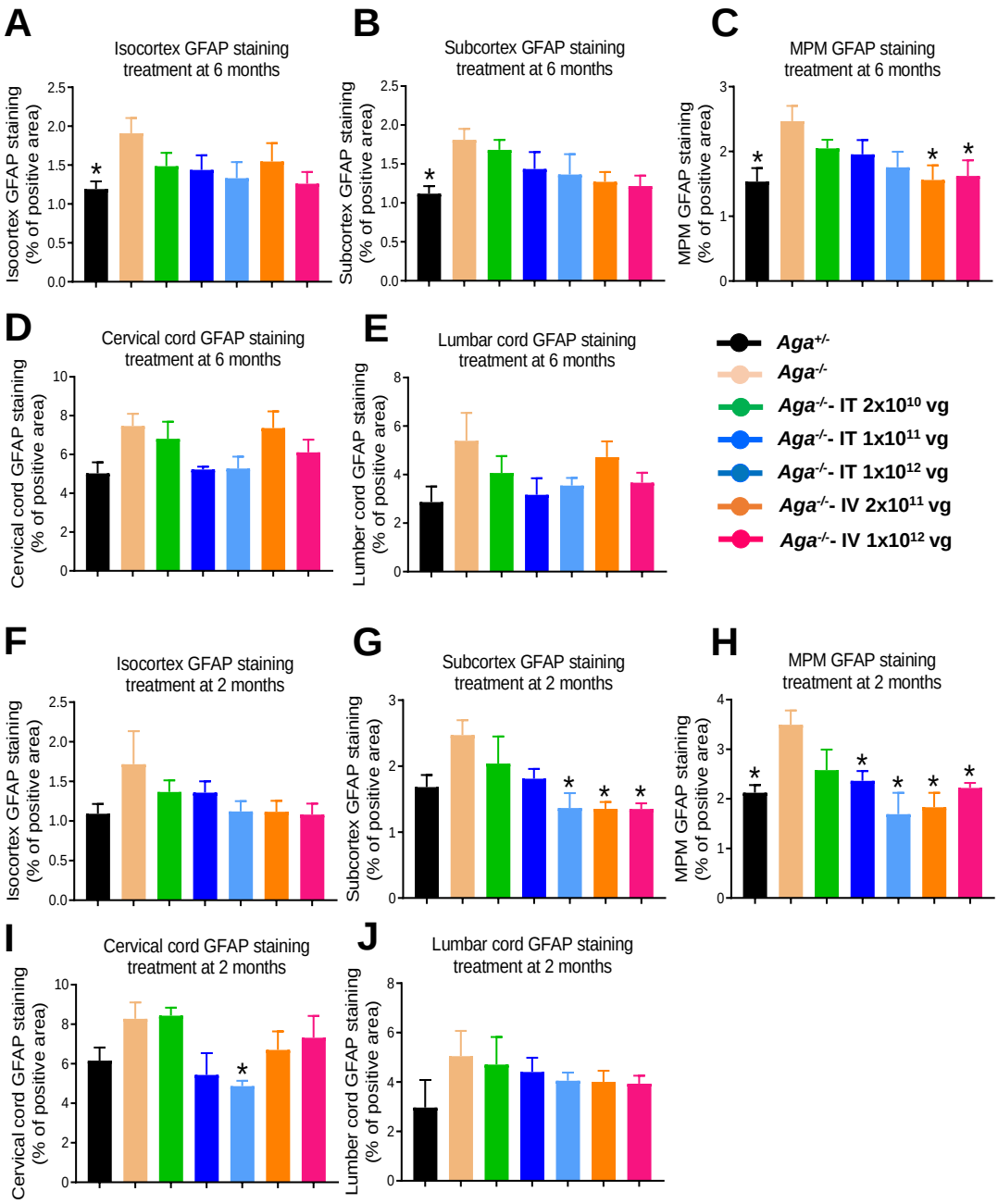

Supplemental Figure 4. AAV9/*AGA* GT reduces gliosis in various part of the CNS in *Aga*$^{-/-}$ mice. Various doses of AAV9/*AGA* vector were administered either IT or IV to *Aga*$^{-/-}$ mice at 6 months old (**A-E**) or 2 months old (**F-J**). At 18 months old, mouse brain was harvested for GFAP staining. All data are presented as mean ± SEM. * depicts significant difference ($p<0.05$) by ordinary one-way ANOVA followed by Dunnett's multiple comparisons test compared to the untreated *Aga*$^{-/-}$ control. Subcortex, hippocampus + thalamus + hypothalamus; MPM, Midbrain + Pons + Medulla. n=5-7 in (**A-E**) and n=4-7 in (**F-J**).

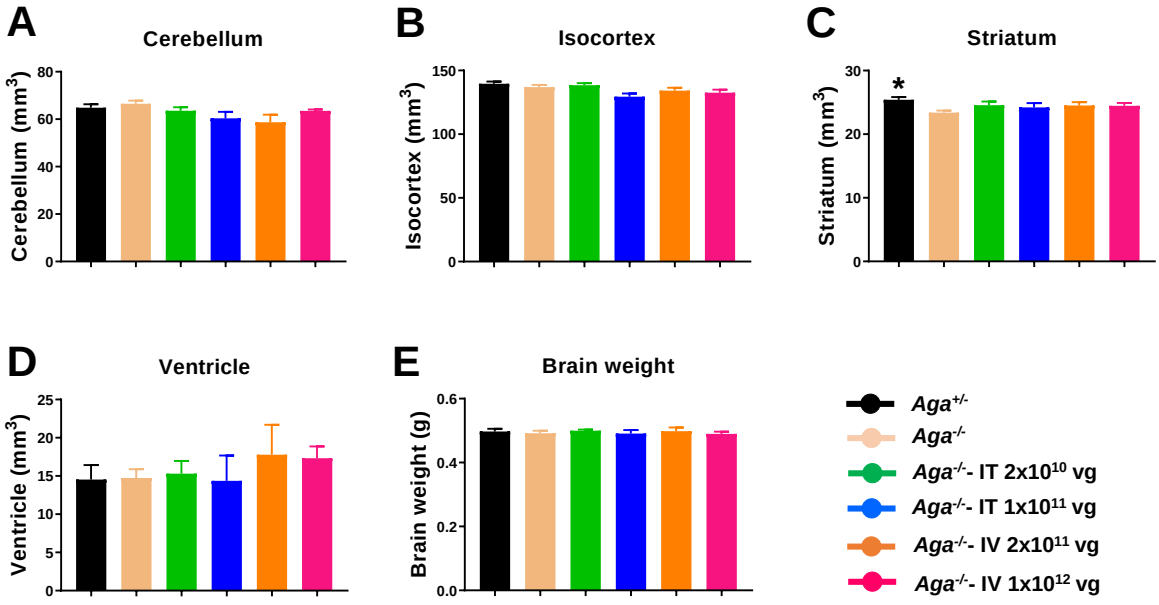

Supplemental Figure 5. There is no significant difference between any groups in terms of brain size (A-D) or brain weight (E). MRI was performed on mice at 16 months old and brain size (**A-D**) was calculated. Brain weight (**E**) was obtained at 18 months old during necropsy. All data are presented as mean ± SEM. Significant difference was performed using ordinary one-way ANOVA followed by Dunnett's multiple comparisons test compared to the untreated *Aga*$^{-/-}$ control. No significant differences were found between any cohorts. n=3-8 in (**A-D**) and n=4-11 in (**E**).

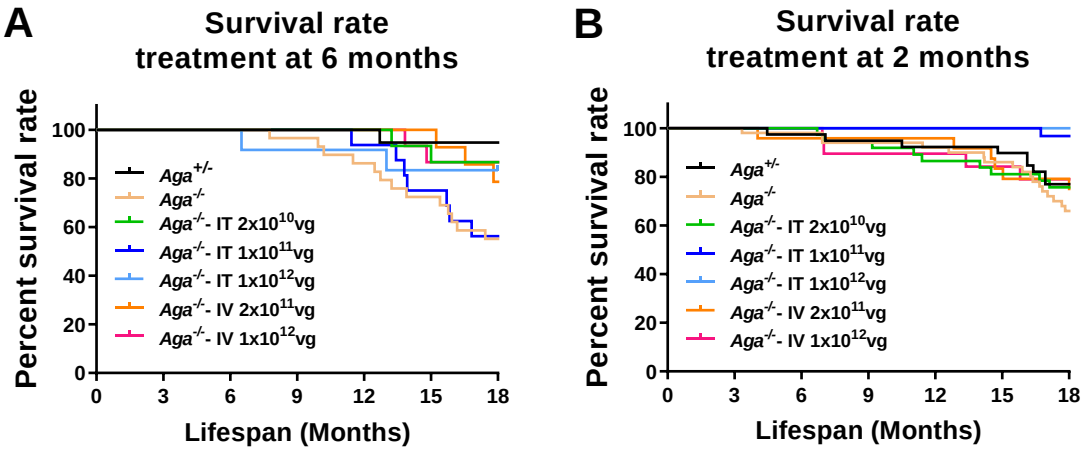

Supplemental Figure 6. AAV9/*AGA* GT does not decrease survival rate in *Aga*$^{-/-}$ mice. Various doses of AAV9/*AGA* vector were administered either IT or IV to *Aga*$^{-/-}$ mice at 6 months old (**A**) or 2 months old (**B**). Significant difference was analyzed via log-rank [Mantel Cox] test. No significant differences were found between any cohorts. n=12-29 in (**A**) and n=15-50 in (**B**).

Supplemental Quality Control Summary

UNIVERSITY OF NORTH CAROLINA
VECTOR CORE

Quality Control Summary

Lot #		LAV9

Test by qPCR

Test #	Titer, vg/mL	Analyst	Date	File
1	1.11E+13	PZ	08/9/2016	20160809-1634-gh-pz

PAGE analysis

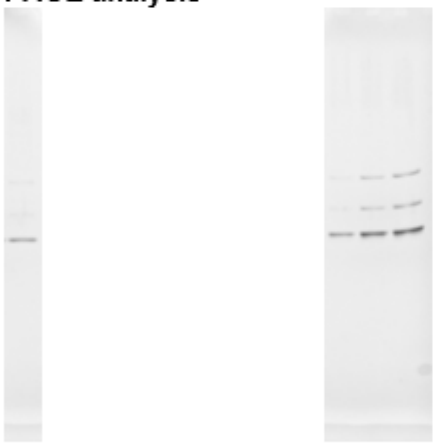

Loaded 5.00E+09 vg PV021 std 2e9vg 5e9vg 1e10vg
Calculated 2.50E+09 vg

Analyst	Ali Hernandez
Date	08/16/2016
Reference #	20160816-silver

UNIVERSITY OF NORTH CAROLINA
VECTOR CORE

SEM

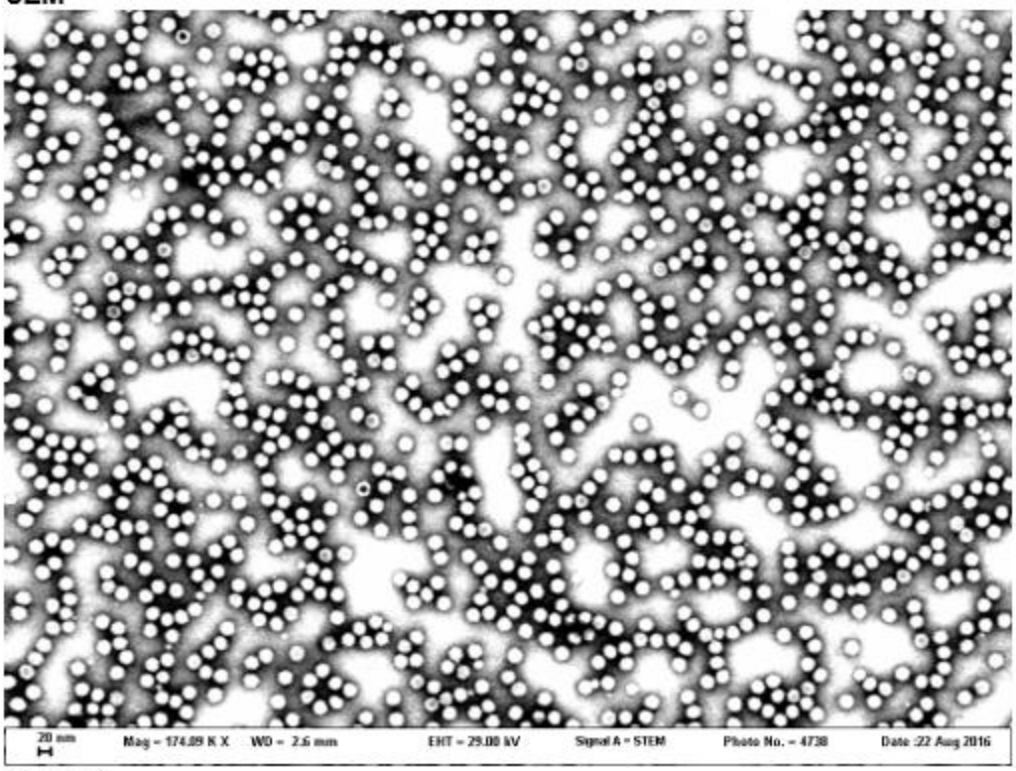

94% full

Analyst	Ali Hernandez
Date	08/22/2016
Reference #	20160822-LAV9-T17-02

University of Texas Southwestern Medical Center
5323 Harry Hines Boulevard
Dallas, Texas 75390
Phone 214-648-1402
Mary.Wight-Carter@UTSouthwestern.edu

FINAL REPORT

Safety Study of scAAV9/AGA Vectors in AGA Knock-out and Heterozygous mice

Report No. 18-088

Sponsor Name:	Rare Trait Hope Fund
Study Director:	Steven Gray, PhD
Contract Pathologist:	Mary Wight-Carter, DVM, DACVP
Date of Final Report:	April 15, 2019

Mary Wight-Carter, DVM, DACVP Date

University of Texas Southwestern Medical Center
5323 Harry Hines Boulevard
Dallas, Texas 75390
Phone 214-648-1402
Mary.Wight-Carter@UTSouthwestern.edu

Table of Contents

List of Tables

University of Texas Southwestern Medical Center
5323 Harry Hines Boulevard
Dallas, Texas 75390
Phone 214-648-1402
Mary.Wight-Carter@UTSouthwestern.edu

1. OBJECTIVE

The objective for this study was to evaluate the safety of long-term high-levels of systemic expression of scAAV9/AGA Vectors in AGA Knock-out mice. These mice were injected intrathecally (IT) at 6 or 2 months old with $1x10^{12}$ vg/mouse of scAAV/AGA vectors. Age- and sex-matched mice were injected with vehicle and maintained as part of the study cohort for comparison.

2. ABBREVIATIONS

AAV	Adeno-Associated Virus
AGU	Aspartylglucosaminuria
AGA KO	AGA Knock-out mouse, animal model for AGU disease
Het	Heterozygous, mice that carry the mutation in one allele but exhibit normal phenotype
AGA	Aspartylglucosaminidase
vg	Vector genomes

3. MATERIALS AND METHODS

Experimental Design: In the current study, AGA Knock-out mice were injected intrathecally (IT) at 6 or 2 months old with $1x10^{12}$ vg/mouse of scAAV/AGA vectors. Age- and sex-matched mice were injected with vehicle and maintained as part of the study cohort for comparison.

The in-life portion of the study was performed in the laboratory of Dr. Gray at the University of North Carolina at Chapel Hill. Postmortem analysis was conducted at the University of Texas Southwestern Medical Center. The work was not conducted in full compliance with the Good Laboratory Practice (GLP) regulations for nonclinical studies (21 CFR Part 58). Animals were grouped and analyzed as detailed in the table below.

University of Texas Southwestern Medical Center
5323 Harry Hines Boulevard
Dallas, Texas 75390
Phone 214-648-1402
Mary.Wight-Carter@UTSouthwestern.edu

Table 1. Study design for safety of scAAV9/AGA vectors in AGA Knock-out mice.

Genotype	Route	Treatment Age (months)	Volume injected (uL)	Dose (vg/mouse)	Viral Source	Number of mice injected	Body weight /survival	Endpoint[b]
AGA Het	-	6	-	-	N/A	4	Yes	18 months old
AGA KO	IT[a]	6	5	Vehicle	UNC-VC	4	Yes	18 months old
AGA KO	IT	6	5	$1x10^{12}$	UNC-VC	4	Yes	18 months old
AGA Het	-	2	-	-	N/A	4	Yes	18 months old
AGA KO	IT	2	5	Vehicle	UNC-VC	4	Yes	18 months old
AGA KO	IT	2	5	$1x10^{12}$	UNC-VC	4	Yes	18 months old

[a] IT: Intrathecal injection through lumber spinal cord. [b] Mice were sacrificed at 18 months of age for histopathology and compared to 4 age- and sex-matched mice.

Tissues were stored in 70% ETOH, trimmed into tissue cassettes and sent for processing to IDEXX laboratories. Hematoxylin and Eosin stained slides were produced from the cassettes. Tissues and the corresponding slides were labeled with the following ID's: 254.19, 264.80, 264.81, 264.86, 222.23, 222.26, 223.30, 223.31, 224.34, 224.35, 224.36, 224.39, 232.81, 232.82, 232.88, 234.97, 254.18, 255.29, 261.58, 261.60, 261.63, 267.00, 268.10, and 273.44. Brain, heart, liver, lung, gonad, spleen, kidney, sciatic nerve, cervical and lumbar spinal cord were submitted for all animals except for the following instances. The sciatic nerve was not present for animal ID 222.26, 224.35, 222.23, 223.30, 224.34, 232.81, 223.31, 234.97, 268.10, 273.44, 261.58, and 264.80. The gonad was not present for animal ID 224.35, 222.23, and 223.30. The lungs, kidney and spleen were also missing for animal ID 224.35 and 223.30.

4. RESULTS AND DISCUSSION

The cerebrum and olfactory bulb of all the mice were microscopically normal. There were no abnormalities found in the cervical or lumbar cord of the mice. There were no abnormalities found in the sciatic nerves in any of the mice.

There was a mild to moderate decrease in the number of Purkinje cells in at least one lobe and occasionally multiple lobes of the cerebellum from mouse numbers 222.23, 223.30, 223.31, 224.34, 224.36, 232.81, 234.97, 267.00, and 273.44.

The seminiferous tubules of animal ID 224.36, 254.18 and 261.58 had multiple variably sized vacuoles that replaced various levels of the seminiferous epithelium in a few tubules. There was no evidence of accompanying germ cell degeneration. Since there were a very few tubules affected and there was no accompanying degeneration, it suggests that this was an incidental finding. No other lesions were present in the mouse testicles.

All of the ovaries that were present were normal and the structures within the ovaries were consistent with various points in the estrus cycle.

The hearts of animal ID 254.18, 261.58, 261.63, 267.00, 224.36, 232.88 and 261.60 had multifocal areas with separation of cardiomyocytes by increased collagen fibers (fibrosis). The areas of fibrosis affected 5-15% of the heart in all instances except for 261.58 and 261.63. 261.58 and 261.63 had approximately 40% of the heart affected. The remainder of the hearts were normal. There was no evidence of heart failure in the other organs, so these degenerative changes were not clinically significant.

The kidneys of 232.81 and 254.19 showed multifocal mild to moderate thickening of the glomerular tufts, multifocal tubular regeneration, mild multifocal interstitial fibrosis, mild to moderate multifocal interstitial and perivascular infiltrates with mononuclear cells (glomerulonephropathy). The multiple glomerular tufts were thickened with eosinophilic proteinaceous material in kidneys of 264.80 (mild glomerulopathy). The kidneys of 264.80 and 261.63 had mild multifocal interstitial fibrosis, with tubular regeneration and mild perivascular infiltrates with small to moderate numbers of mononuclear cells.

There was mild to moderate perivascular infiltrates with small to moderate numbers of mononuclear cells in kidneys of 261.60, 264.86, 254.18, 273.44, 223.31, 224.34, 261.58, and 267.00. There were mild multifocal peripelvic infiltrates with small to moderate numbers of mononuclear cells in kidneys of 224.36, 234.97, 264.80, 222.26, 224.39, 255.29, 268.10, and 232.88.

The tubules of kidneys of 224.36 had a few small areas of mineralization. The renal pelvis had mild to moderate dilation of a few tubules of kidneys of 264.80, 264.86, 224.34, 232.82, 232.88, and 268.10. The above described lesions are not uncommon in adult or aged mice and typically are more frequent in male mice.

The renal pelvis of 255.29 contained a focal area of tubular hyperplasia. This is an incidental finding with no evidence of cellular atypia as would be expected with a neoplastic process.

The livers of the following mice had mild to moderate peribiliary infiltrates with mononuclear cells with no corresponding fibrosis or hepatocellular necrosis: 264.80, 267.00, and 273.44. Minimal to moderate peribiliary and perivascular infiltrates are a common finding in mice and increase in incidence as the mice age.

The livers of the following mice contained multifocal infiltrates with small numbers of mixed inflammatory cell infiltrates with hepatocellular necrosis (micro-abscess): 264.81, 224.34, 232.82, 232.88, 254.18, 261.63, and 267.00. Areas with 1-2 cell hepatocyte necrosis accompanied by inflammatory cells can occur spontaneously in the mouse liver with increased incidence as the mice age.

Animal numbers 223.31 and 232.81 had multifocal areas of extramedullary hematopoiesis present in the liver parenchyma. This is less common in rodents as they age and typically occurs in response to increased hematopoietic demand.

Animal 232.88, 254.18, and 261.63 had a liver nodule grossly which microscopically was morphologically consistent with a hepatocellular adenoma which expanded the parenchyma and compressed the adjacent normal tissue. Adenomas are common findings in adult B6 mice.

Multifocal hepatocytes throughout the livers from 264.80, 264.86, 222.26, 223.31, 224.34, 232.88, 254.18, 255.29, and 261.60 had round variably sized intracytoplasmic vacuoles that are morphologically consistent with lipidosis.

The liver of mouse 254.19 was diffusely infiltrated with a histiocytic sarcoma. Mouse 261.60 had a focal island of tumor tissue that was morphologically consistent with histiocytic sarcoma. This is not an uncommon tumor of older mice on a B6 background.

The lungs from the following mice had mild to moderate perivascular infiltrates with mononuclear cells: 254.19, 264.81, 224.36, 234.97, 254.18, 261.58, 267.00, and 268.10. The lungs from the following mice had mild to moderate peribronchiolar infiltrates with mononuclear cells: 222.23, 222.26, 223.31, 232.81, 232.82, 232.88, and 273.44. These infiltrates are commonly seen in the lungs of adult mice.

Mouse 264.80 had multifocal airways with multiple eosinophilic crystals. Mouse 224.36 and 267.00 had a focal area of acidophilic macrophage pneumonia in which the eosinophilic crystals are within macrophages in the alveoli. This lesion is a common idiopathic finding disease in mice on a B6 background.

Mouse 224.34 had a focal bronchoalveolar adenoma. The alveoli in mouse 232.82 contained multifocal islands of neoplastic small lymphocytes (Lymphoma).

The spleen of all mice had variable amounts of extramedullary hematopoiesis and hemosiderin within the macrophages of the red pulp. This is considered normal in older mice. Mouse 232.82 had enlarged spleens grossly and the white pulp was expanded with neoplastic small lymphocytes. (Lymphoma). The spleen of 223.31 was moderately enlarged grossly and the white pulp was diffusely hyperplastic.

5. CONCLUSIONS

The tumors, increased number of inflammatory cell infiltrates and degenerative lesions within multiple organs that were seen are considered to be common background lesions in aged mice. None of the microscopic findings are suggestive of adverse effects related to vector administration in these mice.

University of Texas Southwestern Medical Center
5323 Harry Hines Boulevard
Dallas, Texas 75390
Phone 214-648-1402
Mary.Wight-Carter@UTSouthwestern.edu

6. APPENDIX – HISTOPATHOLOGIC FINDINGS IN INDIVIDUAL MICE

Tissues were reviewed by a pathologist that was blinded to the study groups. The tumors and increased number of inflammatory cell infiltrates and degenerative lesions seen in these mice are expected in mice as they age.

Genotype	AGA Het				AGA KO					AGA KO				
Treatment Age (months)	6				6					6				
Dose (vg/mouse)	N/A				Vehicle					$1x10^{12}$				
Mouse ID	222.26	224.35	224.39	232.82	222.23	223.30	224.34	232.81	224.36	232.88	223.31	234.97		
Gender	M	M	F	F	M	M	F	F	M	M	F	F		
Gross finding				Splenomegaly	enlarged bladder	enlarged bladder		enlarged fallopian tube		liver nodule	splenomegaly			
cerebrum	normal	normal	normal	normal		normal	normal	normal	normal	normal	normal	normal		
cerebellum: mild to moderate decrease in the number of Purkinje cells in at least one lobe and occasionally multiple lobes of the cerebellum	normal	normal	normal	normal	x	x	x	x	x	normal	x	x		
olfactory bulb	normal	normal	normal	normal		normal	normal	normal	normal	normal	normal	normal		
cervical cord	normal	normal	normal	normal		normal	normal	normal	normal	normal	normal	normal		
lumbar cord	normal	normal	normal	normal		normal	normal	normal	normal	normal	normal	normal		
sciatic nerve	no data	no data	normal	normal	no data	no data	no data	no data	normal	normal	no data	no data		
ovaries			normal	normal			normal	normal			normal	normal		
testicles: multiple variably sized vacuoles, which is an incidental finding		no data			no data	no data			x					
heart: multifocal areas with separation of cardiomyocytes by increased collagen fibers (fibrosis), which were not clinically significant.									x	x				
kidney: multifocal mild to moderate thickening of the glomerular tufts, multifocal tubular regeneration, mild multifocal interstitial fibrosis, mild to moderate multifocal interstitial and perivascular infiltrates with mononuclear cells (glomerulonephropathy), which is not uncommon in adult or aged mice								x						
kidney: multiple glomerular tufts were thickened with eosinophilic proteinaceous material (mild glomerulopathy), which is not uncommon in adult or aged mice														
kidney: mild multifocal interstitial fibrosis, with tubular regeneration and mild perivascular infiltrates with small to moderate numbers of mononuclear cells														
kidney: moderate perivascular infiltrates with small to moderate numbers of mononuclear cells, which is not uncommon in adult or aged mice							x				x			
kidney: mild multifocal peripelvic infiltrates with small to moderate numbers of mononuclear cells, which is not uncommon in adult or aged mice	x		x						x	x		x		
Kidney: a few small areas of mineralization in the tubules, which is not uncommon in adult or aged mice									x					
kidney: mild to moderate dilation of a few tubules, which is not uncommon in adult or aged mice				x			x			x				
kidney: a focal area of tubular hyperplasia in renal pelvis, an incidential finading														
liver: mild to moderate peribiliary infiltrates with mononuclear cells with no corresponding fibrosis or hepatocellular necrosis, which is a common finding in mice and increase in incidence as the mice age														
liver: multifocal infiltrates with small numbers of mixed inflammatory cell infiltrates with hepatocellular necrosis (micro-abscess), which occurs spontaneously in the mouse liver with increased incidence as the				x			x			x				
liver: multifocal areas of extramedullary hematopoiesis present in the liver parenchyma, which is less common in rodents as they age and typically occurs in response to increased hematopoietic demand								x			x			
liver: hepatocellular adenoma which expanded the parenchyma and compressed the adjacent normal tissue. Adenomas are common findings in adult B6 mice										x				
liver: round variably sized intracytoplasmic vacuoles that are morphologically consistent with lipidosis	x						x			x	x	x		
liver: histiocytic sarcoma, which is not an uncommon tumor of older mice on a B6 background														
lung: moderate perivascular infiltrates with mononuclear cells, which are commonly seen in the lungs of adult mice									x			x		
lung: mild to moderate peribronchiolar infiltrates with mononuclear cells, which are commonly seen in the lungs of adult mice	x			x	x			x		x	x			
lung: multifocal airways with multiple eosinophilic crystals, a common idiopathic finding disease in B6 mice									x					
lung: a focal bronchoalveolar adenoma							x							
lung: multifocal islands of neoplastic small lymphocytes (Lymphoma) in the alveoli				x										
spleen: white pulp was expanded with neoplastic small lymphocytes. (Lymphoma).				x										
spleen: white pulp was diffusely hyperplastic												x		

University of Texas Southwestern Medical Center
5323 Harry Hines Boulevard
Dallas, Texas 75390
Phone 214-648-1402
Mary.Wight-Carter@UTSouthwestern.edu

Genotype	AGA Het				AGA KO				AGA KO			
Treatment Age (months)	2				2				2			
Dose (vg/mouse)	N/A				Vehicle				$1x10^{12}$			
Mouse ID	254.18	261.60	254.19	264.80	261.63	267.00	268.10	273.44	255.29	261.58	264.81	264.86
Gender	M	M	F	F	M	M	F	F	M	M	F	F
Gross finding	liver nodule		heptosplenomegaly		liver nodule		spleen lesion					
cerebrum	normal	normal	normal	normal	normal	normal	normal	normal	normal	normal	normal	normal
cerebellum: mild to moderate decrease in the number of Purkinje cells in at least one lobe and occasionally multiple lobes of the cerebellum	normal	normal	normal	normal	normal	x	normal	x	normal	normal	normal	normal
olfactory bulb	normal	normal	normal	normal	normal	normal	normal	normal	normal	normal	normal	normal
cervical cord	normal	normal	normal	normal	normal	normal	normal	normal	normal	normal	normal	normal
lumbar cord	normal	normal	normal	normal	normal	normal	normal	normal	normal	normal	normal	normal
sciatic nerve	normal	normal	normal	no data	normal	normal	no data	no data	normal	no data	normal	normal
ovaries			normal	normal			normal	normal			normal	normal
testicles: multiple variably sized vacuoles, which is an incidental finding	x									x		
heart: multifocal areas with separation of cardiomyocytes by increased collagen fibers (fibrosis), which were not clinically significant.	x	x			x	x				x		
kidney: multifocal mild to moderate thickening of the glomerular tufts, multifocal tubular regeneration, mild multifocal interstitial fibrosis, mild to moderate multifocal interstitial and perivascular infiltrates with mononuclear cells (glomerulonephropathy), which is not uncommon in adult or aged mice			x									
kidney: multiple glomerular tufts were thickened with eosinophilic proteinaceous material (mild glomerulopathy), which is not uncommon in adult or aged mice				x								
kidney: mild multifocal interstitial fibrosis, with tubular regeneration and mild perivascular infiltrates with small to moderate numbers of mononuclear cells				x	x							
kidney: moderate perivascular infiltrates with small to moderate numbers of mononuclear cells, which is not uncommon in adult or aged mice	x	x				x		x		x		x
kidney: mild multifocal peripelvic infiltrates with small to moderate numbers of mononuclear cells, which is not uncommon in adult or aged mice				x			x		x			
Kidney: a few small areas of mineralization in the tubules, which is not uncommon in adult or aged mice												
Kidney: mild to moderate dilation of a few tubules, which is not uncommon in adult or aged mice				x			x					x
kidney: a focal area of tubular hyperplasia in renal pelvis, an incidential finading									x			
liver: mild to moderate peribiliary infiltrates with mononuclear cells with no corresponding fibrosis or hepatocellular necrosis, which is a common finding in mice and increase in incidence as the mice age				x		x		x				
liver: multifocal infiltrates with small numbers of mixed inflammatory cell infiltrates with hepatocellular necrosis (micro-abscess), which occurs spontaneously in the mouse liver with increased incidence as the	x				x	x					x	
liver: multifocal areas of extramedullary hematopoiesis present in the liver parenchyma, which is less common in rodents as they age and typically occurs in response to increased hematopoietic demand												
liver: hepatocellular adenoma which expanded the parenchyma and compressed the adjacent normal tissue. Adenomas are common findings in adult B6 mice	x				x							
liver: round variably sized intracytoplasmic vacuoles that are morphologically consistent with lipidosis	x	x		x					x			x
liver: histiocytic sarcoma, which is not an uncommon tumor of older mice on a B6 background		x	x									
lung: moderate perivascular infiltrates with mononuclear cells, which are commonly seen in the lungs of adult mice	x		x			x	x			x	x	
lung: mild to moderate peribronchiolar infiltrates with mononuclear cells, which are commonly seen in the lungs of adult mice								x				
lung: multifocal airways with multiple eosinophilic crystals, a common idiopathic finding disease in B6 mice				x		x						
lung: a focal bronchoalveolar adenoma												
lung: multifocal islands of neoplastic small lymphocytes (Lymphoma) in the alveoli												
spleen: white pulp was expanded with neoplastic small lymphocytes. (Lymphoma).												
spleen: white pulp was diffusely hyperplastic												